AIRCRAFT DIGITAL CONTROL DESIGN METHODS

by

J. David Powell, Principal Investigator

Eric Parsons, Research Assistant

Michael G. Tashker, Stanford Research Institute

Guidance and Control Laboratory

Department of Aeronautics and Astronautics

Stanford University

Stanford, California 94305

February 1976

FINAL REPORT

ABSTRACT

Many variations in design methods for aircraft digital flight control have been proposed in the literature. In general, the methods fall into two categories; those where the design is done in the continuous domain (or s-plane) and those where the design is done in the discrete domain (or z-plane). This report evaluates several variations of each category and compares them for various flight control modes of the Langley TCV Boeing 737 aircraft. Design method fidelity is evaluated by examining closed loop root movement and the frequency response of the discretely controlled continuous aircraft. It was found that all methods provided acceptable performance for sample rates greater than 10 cps except the "uncompensated s-plane design" method which was acceptable above 20 cps. A design procedure based on optimal control methods was proposed that provided the best fidelity at very slow sample rates and required no design iterations for changing sample rates.

At very slow sample rates, system roughness or jerkiness may be the limiting factor on the design. To better understand this phenomenon, an experimental study was defined for the Langley motion simulator with candidate designs for evaluation.

TABLE OF CONTENTS

Abstract

1.0 Introduction

Digital Computers for aircraft inner-loop control functions have been implemented for research purposes[1,2] and will probably be used for operational aircraft within the next few years. This research has been carried out in order to facilitate the design and performance evaluation of discrete flight control systems for future missions.

Many variations in design methods exist, but generally fall into two broad categories: 1) those where the design is done in the continuous domain (or s-plane) and then discretized, and 2) those where the design is done in the discrete domain (z- or w-plane).

Design using the first category is attractive since it utilizes the experience gained over many years of continuous autopilot design, and the additional discretization step required can be separated from the s-plane design process. All the discretization procedures (z-transform, bilinear or Tustin's, and z-forms) introduce an error[3] which is small for relatively fast sampling (typically > 40 Hz) but grows larger as the sample rate is reduced. The effect of this error or approximation in the design method is generally checked by a simulation of the system. In some cases, a continuous control design exists and the sole requirement on the designer is to obtain the software for the digital computer which duplicates the continuous control as closely as possible. For these cases, only the discretization and verification via simulation is required.

Design using the second category includes the w plane techniques,[4,5] z-plane Nyquist techniques,[6] and discrete state space techniques.[7,8,9] These methods do not introduce an error due to the discrete nature of the problem at any sample rate and therefore are particularly attractive when attempting to establish the lowest practical sample rate.

There is an interaction between the design method sample rate, system sensitivity, roughness of control, prefilter design, and gust response that needs to be thoroughly understood in order to synthesize digital control systems with confidence. Preliminary results[9] on the interaction between the sample rate and system sensitivity and gust

response for a high performance aircraft indicate that sample rates can be used which are lower than those typically judged necessary in previously reported aircraft digital control studies.[1,10,11,12] This research primarily concerns design method evaluations as a function of sample rate. Preliminary results concerning roughness of control are also included.

2.0 Design Methods

2.1 Introduction

The following sections carry out discrete designs for the NASA TCV Boeing 737 autopilot using several different methods. All the resulting designs are checked using an exact discrete analysis to determine the fidelity of the design method vs. sample rate.

Although only a few autopilot modes have been studied, the dynamics of the aircraft in the remaining modes of the autopilot are not sufficiently different to cause any significant change in the results concerning design methods. However, for other aircraft with significantly faster natural modes or greater structural flexibility, the results contained here do not apply.

2.2 Digitized S-Plane Design

Digitized s-plane design refers to the one-for-one replacement of continuous transfer function blocks with difference equations that can be mechanized on a digital computer. In classical flight control designs, these blocks fall into 4 general categories: integrators, washouts, simple lag networks, and compound lead or lag shaping networks for frequency compensation. The systems being considered here are ones that feed back sensor signals (from accelerometers, gyros, altimeters, etc.) which have been processed through these networks for stability improvement, or noise or bias rejection.

The digital problem after s-plane synthesis of an appropriate control is to obtain the best possible match of a continuous compensator with a digital filter. There are many methods of transforming a continuous filter into digital form [Refs. 13, 14, 15, 16] among which are the direct method, impulse invariant, zero-order hold, bilinear approximation (sometimes called Tustin's method), and the matched z-transform. The most successful methods exactly map the poles and zeros of the continuous filter into the z-plane by the transformation $z = e^{st}$ for all sampling rates. Some methods, notably Tustin's method without pre-

warping, cause a shift in the poles and zeros of the filter at low sampling rates. Exact mapping of the poles and zeros means that the transformation itself plays less of a part in any degradation of performance of the digital system.

The matched z-transform [16] was used in this analysis. For the continuous filter transfer function,

$$G(s) = \frac{K \prod_{i=1}^{m} \left(s + \alpha_i \right) \prod_{i=1}^{n} \left[\left(s + a_i \right)^2 + b_i^2 \right]}{\prod_{i=1}^{r} \left(s + \beta_i \right) \prod_{i=1}^{s} \left[\left(s + c_i \right)^2 + d_i^2 \right]}$$

the digital mechanization is

$$G(z) = \frac{K'(z + 1)^k \prod_{i=1}^{m} \left(z - e^{-\alpha_i T} \right) \prod_{i=1}^{n} \left(z^2 - 2e^{-a_i T} \cos b_i Tz + e^{-2a_i T} \right)}{\prod_{i=1}^{r} \left(z - e^{-\beta_i T} \right) \prod_{i=1}^{s} \left(z^2 - 2e^{-c_i T} \cos d_i Tz + e^{-2c_i T} \right)}$$

where

$$k = r + 2s - m - 2n, \quad k \geq 0$$

and K' is the normalization constant. K' can be chosen to produce the desired gain at either high or low frequency. Thus, to choose the gain at low frequency, $G(z)$ is evaluated at $z = +1$ and K' picked to yield the desired magnitude. For a high frequency gain, $G(z)$ is evaluated at $z = -1$. Table I shows the transforms and associated difference equations for the four forms of compensation mentioned above.

Even though any root movement due to the transformation is eliminated, there is still some degradation of performance due to the physical zero-order hold (ZOH). The hold produces a lag proportional to the sampling interval, and can be regarded as causing a shift in the z-plane zeros of the plant that increases with the sampling interval. This zero shift occurs for all plant zeros not at the origin. Thus, any system whose digital compensation is determined without taking into account the phase shift of the hold mechanization will have degraded performance for long

Transfer Function	Differential Equation	Transform	Difference Equation
$\dfrac{1}{s}$	$\dot{y} = x$	$\dfrac{T}{2}\left(\dfrac{z+1}{z-1}\right)$	$y_n = y_{n-1} + \dfrac{T}{2}\left(x_n + x_{n-1}\right)$
$\dfrac{1}{\tau s+1}$	$\dot{y} = -\dfrac{1}{\tau}y + \dfrac{1}{\tau}x$	$\dfrac{1-e^{-T/\tau}}{2}\left(\dfrac{z+1}{z-e^{-T/\tau}}\right)$	$x_n = e^{-T/\tau}y_{n-1} + \left(\dfrac{1-e^{-T/\tau}}{2}\right)(x_n + x_{n-1})$
$\dfrac{\tau s}{\tau s+1}$	$\dot{q} = -\dfrac{1}{\tau}q + x$ $y = -\dfrac{1}{\tau}q + x$	$\dfrac{1+e^{-T/\tau}}{2}\dfrac{(z-1)}{z-e^{-T/\tau}}$	$x_n = e^{-T/\tau}y_{n-1} + \left(\dfrac{1+e^{-T/\tau}}{2}\right)(x_n - x_{n-1})$
$\dfrac{\tau_1 s+1}{\tau_2 s+1}$	$\dot{q} = -\dfrac{1}{\tau_2}q + \dfrac{1}{\tau_2}x$ $y = \left(1-\dfrac{\tau_1}{\tau_2}\right)q + \dfrac{\tau_1}{\tau_2}x$	$\left(\dfrac{1-e^{-T/\tau_2}}{1-e^{-T/\tau_1}}\right)\left(\dfrac{z-e^{-T/\tau_1}}{z-e^{-T/\tau_2}}\right)$	$y_n = e^{-T/\tau_2}y_{n-1}$ $+ \left(\dfrac{1-e^{-T/\tau_2}}{1-e^{-T/\tau_1}}\right)\left(x_n - e^{-T/\tau_1}x_{n-1}\right)$

Table I

Matched Z transforms for common filters

-5-

sampling intervals (or low sample rates).

Formally, the procedure of digitized s-plane design consists
of transforming an already existing s-plane design by substituting a
difference equation for each control block. A reasonable measure of the
success of this technique is to compare the equivalent s-plane root
locations of the closed loop discrete system at various sampling rates to
the closed loop roots of the continuous system. This comparison is not
a function of the merits of the continuous design; the continuous system
roots are taken to be the desired roots. The consequences of any root
shifting can be displayed graphically by a transient response simulation.
This has been done for three systems based on the TCV Boeing 737:

    1) Pitch SAS,

    2) Pitch attitude control wheel steering,

    3) Longitudinal autoland.

For each of these systems a block diagram of the model[†] will be presented
with the difference equations produced by the digitization, as well as
a locus of root locations. Appropriate transient response plots will
also be shown.

The equivalent s-plane roots of the system with a digital
control law are determined by a method suitable for computer mechanization.
First, the transition matrix is determined from the plant equations of
motion and hold characteristics:

Given

$$\dot{x} = Fx + Gu$$

then $x_{n+1} = \varphi x_n + \Gamma u_n$

where $\varphi = e^{FT}$

$$\Gamma = \int_0^T e^{F\tau} Gd\tau,$$

and T = the sampling interval.

These difference equations are combined with the difference
equations of the controller (put into appropriate state form), and the

---

[†] The models are based on the actual TCV autopilot with nonlinearities
removed.

eigenvalues found. These z-plane eigenvalues are transformed back into
the s-plane by the inverse relation $s = \ell n(z)/T$. A program to perform
these operations as well as certain synthesis methods is described in the
appendix.

2.2.1. Pitch SAS

The pitch SAS is simple pitch rate feedback to the elevator for
better damping and higher bandwidth. A short period model of the airplane
is used here: a block diagram of the continuous system is shown in Figure 1.
In this system it is assumed that the control law is calculated instanta-
neously; there is no sampling interval delay at the output of the controller.
Also note that there is no washout on pitch rate in this model. Although
a washout is common in most stability augmentation systems, it does not
affect root locations or their variation since its break frequency is
quite low. Without the washout, the digital controller has no states and
no difference equation; therefore, this example is somewhat degenerate
but will serve as a basis for comparison with other design metnods in
later sections. The root movement shown in Figure 2 is due entirely to
the lag induced by the ZOH. This lag causes immediate degradation of the
system damping. The real root is very slow and is not affected by
sampling rate.

2.2.2 Pitch Attitude Control-Wheel Steering

The aircraft model for the attitude control-wheel steering mode
is the same as that shown in Figure 1 with the addition of a pitch angle
state. In this mode pitch rate is fed back through a washout to eliminate
any steady-state component. The output of the washout and difference
between the pitch angle and the preselected pitch angle is fed back through
a one cycle delay to simulate computational delay.

The existence of this delay depends on the particular mechanization
and does not always exist. Its presence degrades the stability and per-
formance of the system more than would be encountered without it.

A block diagram of this system is shown in Figure 3.

The continuous washout for the TCV is:

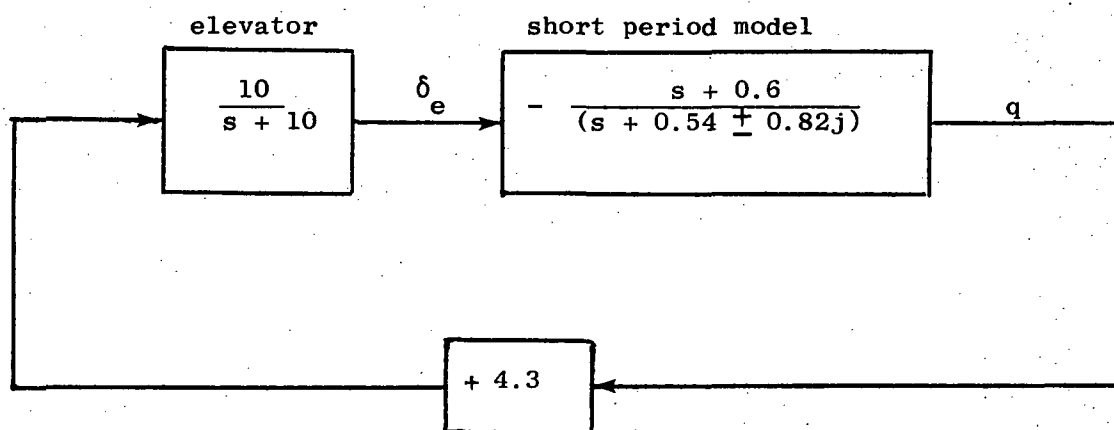$$\frac{d(s)}{c(s)} = \frac{16s}{16s + 1}$$

which yields a discrete transfer function (Table II) of

$$\frac{d(z)}{c(z)} = \frac{1 + e^{-T/16}}{2} \left(\frac{z - 1}{z - e^{-T/16}} \right)$$

and a difference equation

$$d_{n+1} = C_1 d_n + C_2 (c_{n+1} - c_n)$$

where the values of the coefficients are given in Table II for several sample rates.

Short Period model in state space form:

$$\begin{bmatrix} \dot{w} \\ \dot{q} \end{bmatrix} = \begin{bmatrix} -.6283 & 207.1 \\ -.0033 & -.4499 \end{bmatrix} \begin{bmatrix} w \\ q \end{bmatrix} + \begin{bmatrix} -.1408 \\ -.01739 \end{bmatrix} \delta_e$$
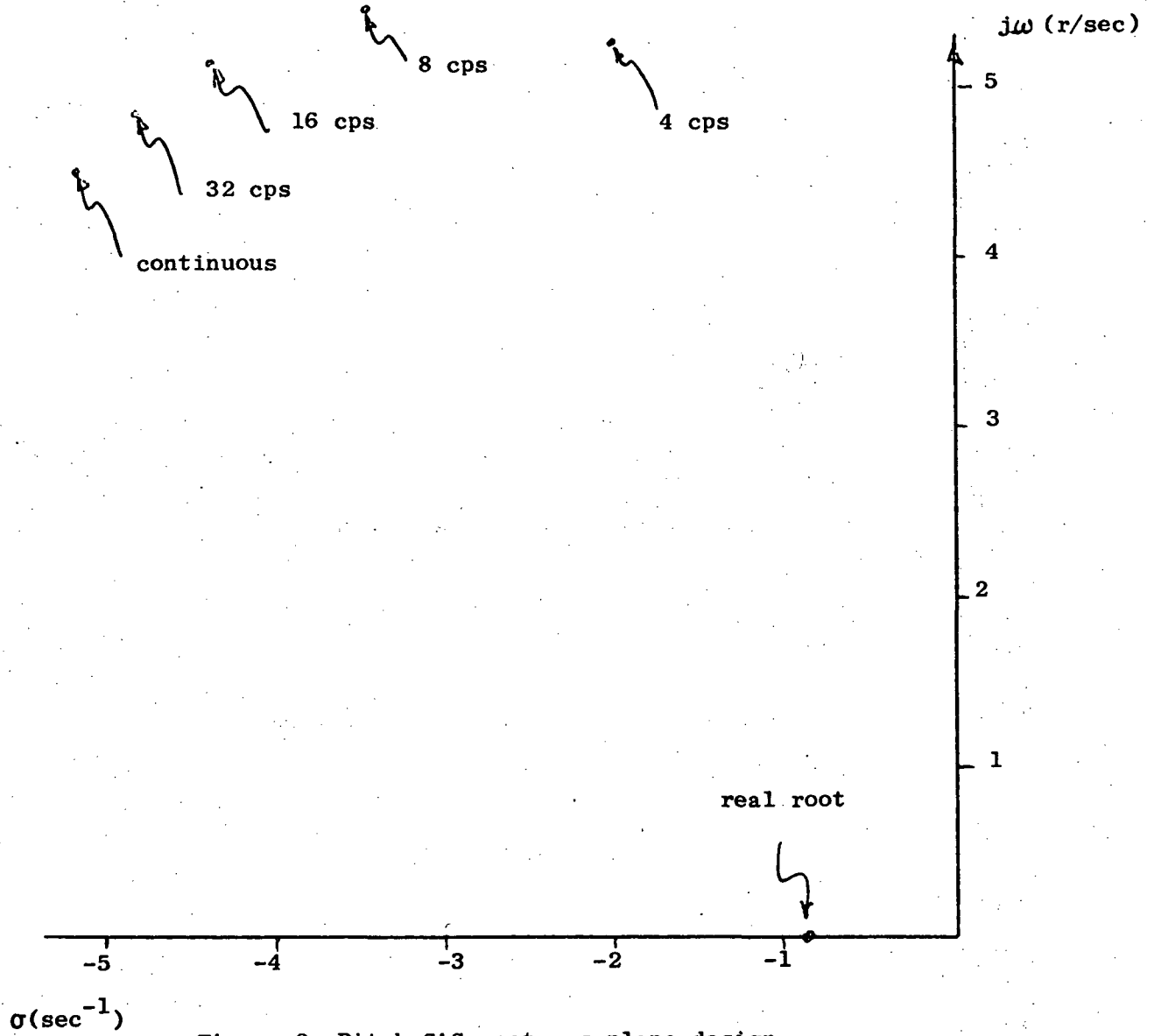
Figure 1   Pitch SAS Model

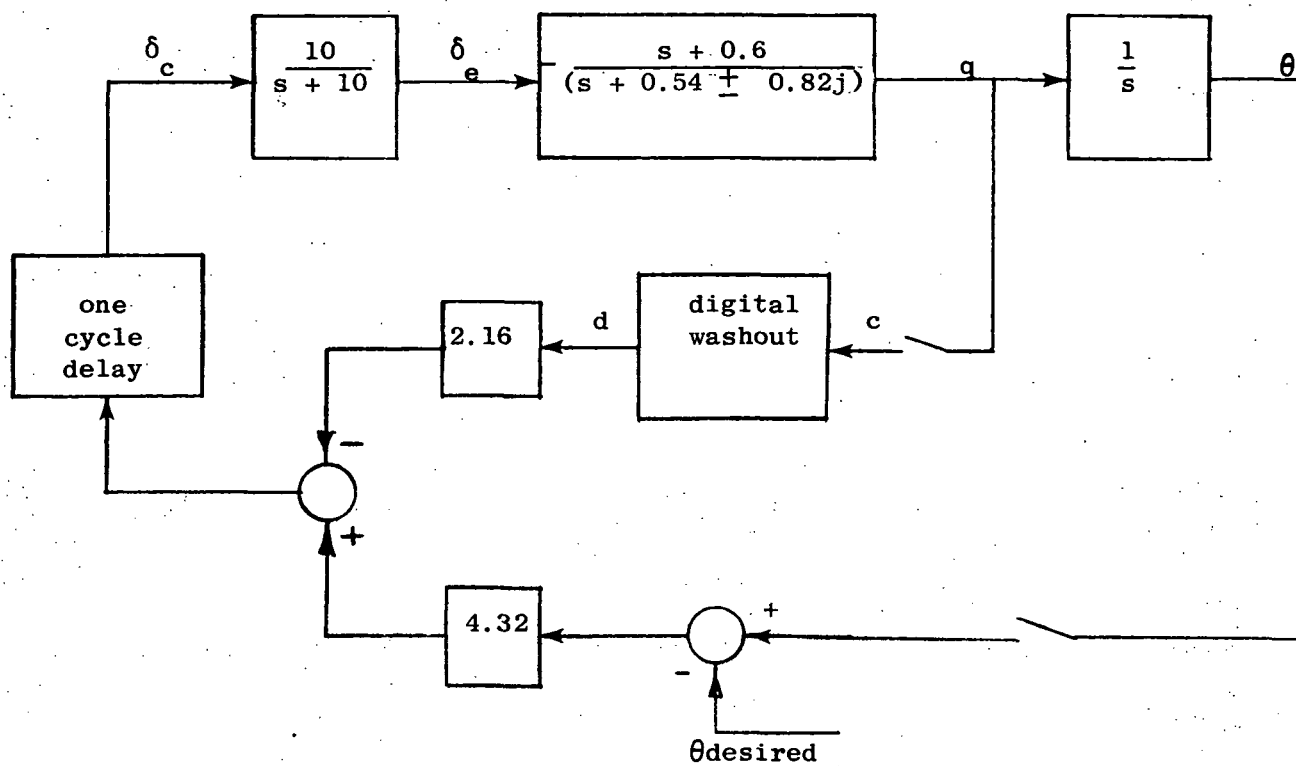Figure 2 Pitch SAS roots, s-plane design

δ_c

$\dfrac{10}{s + 10}$

δ_e

$\dfrac{s + 0.6}{(s + 0.54 \pm 0.82j)}$

q

$\dfrac{1}{s}$

θ

one cycle delay

2.16

d

digital washout

c

−

+

4.32

+

−

θdesired

Figure 3 Pitch Attitude Control Wheel Steering Model

For the purposes of analysis and simulation, the input from the control wheel is assumed to be zero.   The variation in dominant root locations versus sampling rate is shown in Figure 4.   The transient response of pitch angle and pitch rate is shown in Figure 5 for an initial pitch error of 0.1 radian.

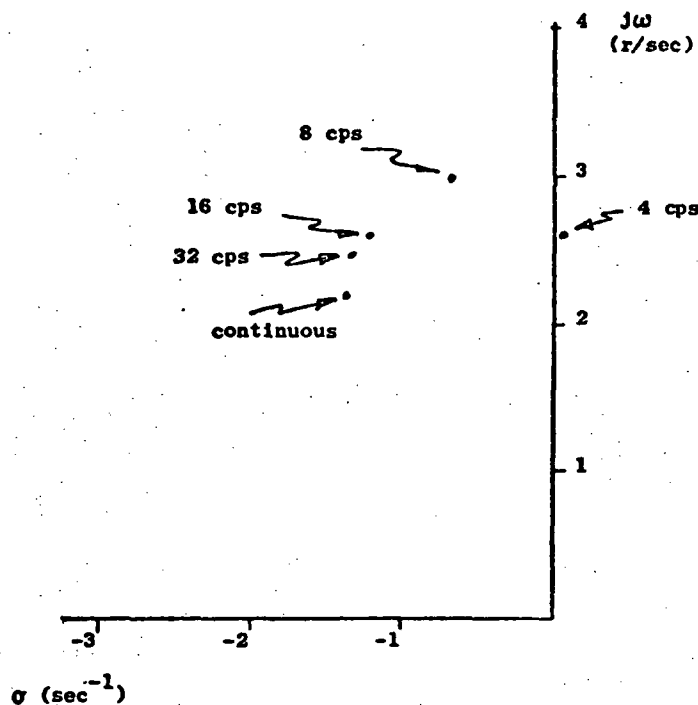Sampling at 4 cps causes instability and is not shown.

Figure 4
Dominant roots of the
Control-wheel steering mode

2.2.3 Longitudinal Autoland

The longitudinal autoland aircraft model is the same as that
for the control-wheel steering model with the addition of a vertical
position state given by:

$$\dot{h} = \dot{w} - 207.1\theta$$

The feedback control (Figure 6) was taken from drawings of the NASA
Langley's TCW Boeing 737 and linearized. As with the control-wheel
steering mode, a one cycle delay is assumed in the controller. The
digital washout coefficients are the same as in Table II while the
difference equation for the digital integration is

$$b_{n+1} = b_n + \frac{T}{2}(a_{n+1} + a_n)$$

-11-
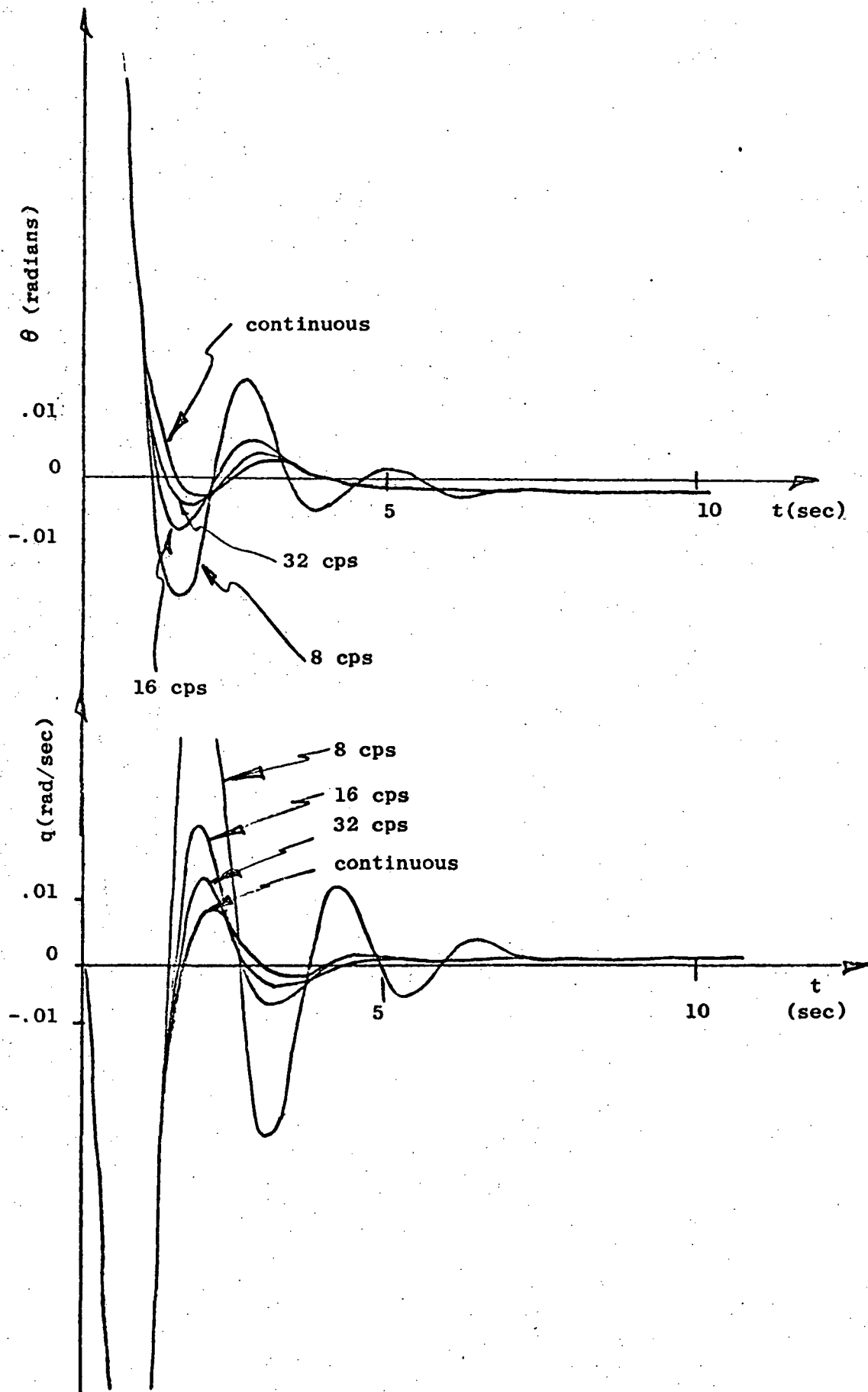
Figure 5 Pitch Angle/Rate, Control Wheel Steering

The variation in dominant root locations versus sampling rate is shown in Figure 7. Figure 8 shows the error in pitch rate for an initial altitude error of 100 feet off the glide slope. Again sampling at 4 cps results in instability.

In summary, digitized s-plane design is suitable for higher sampling rates or for systems with high relative stability. The addition of delays due to computation(which are cascaded in several multi-computer systems) has an increased effect with slower sampling.

q $\xrightarrow{\text{c}}$ | digital washout | $\xrightarrow{\text{d}}$ (5.1)

$\ddot{h}$ ———————→

$\dot{h}$ ——————→ (1.6)

h ——————→ (0.28)

(.0187) $\xrightarrow{\text{a}}$ | digital integration | $\xrightarrow{\text{b}}$

Σ

(.85)
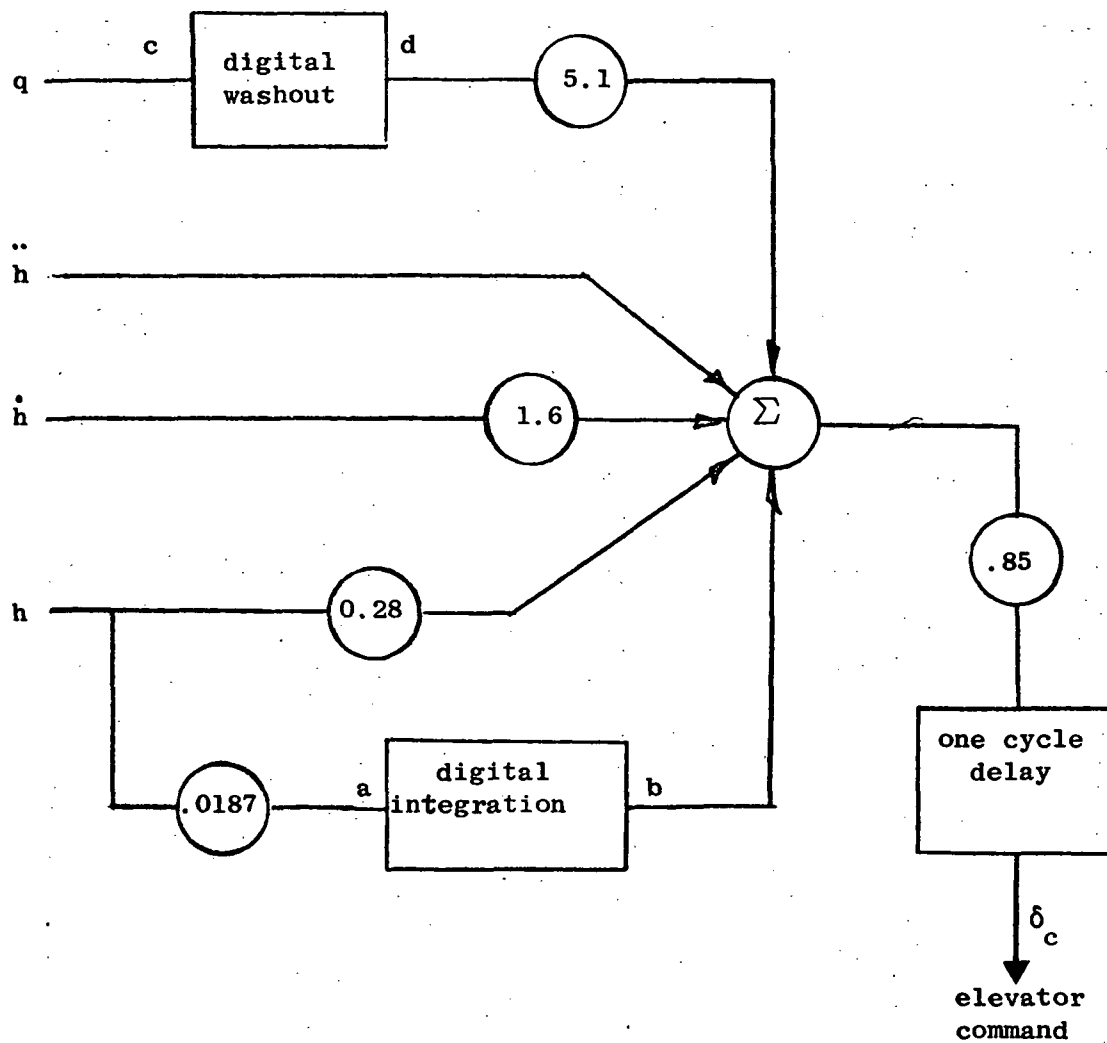
| one cycle delay |

δ_c
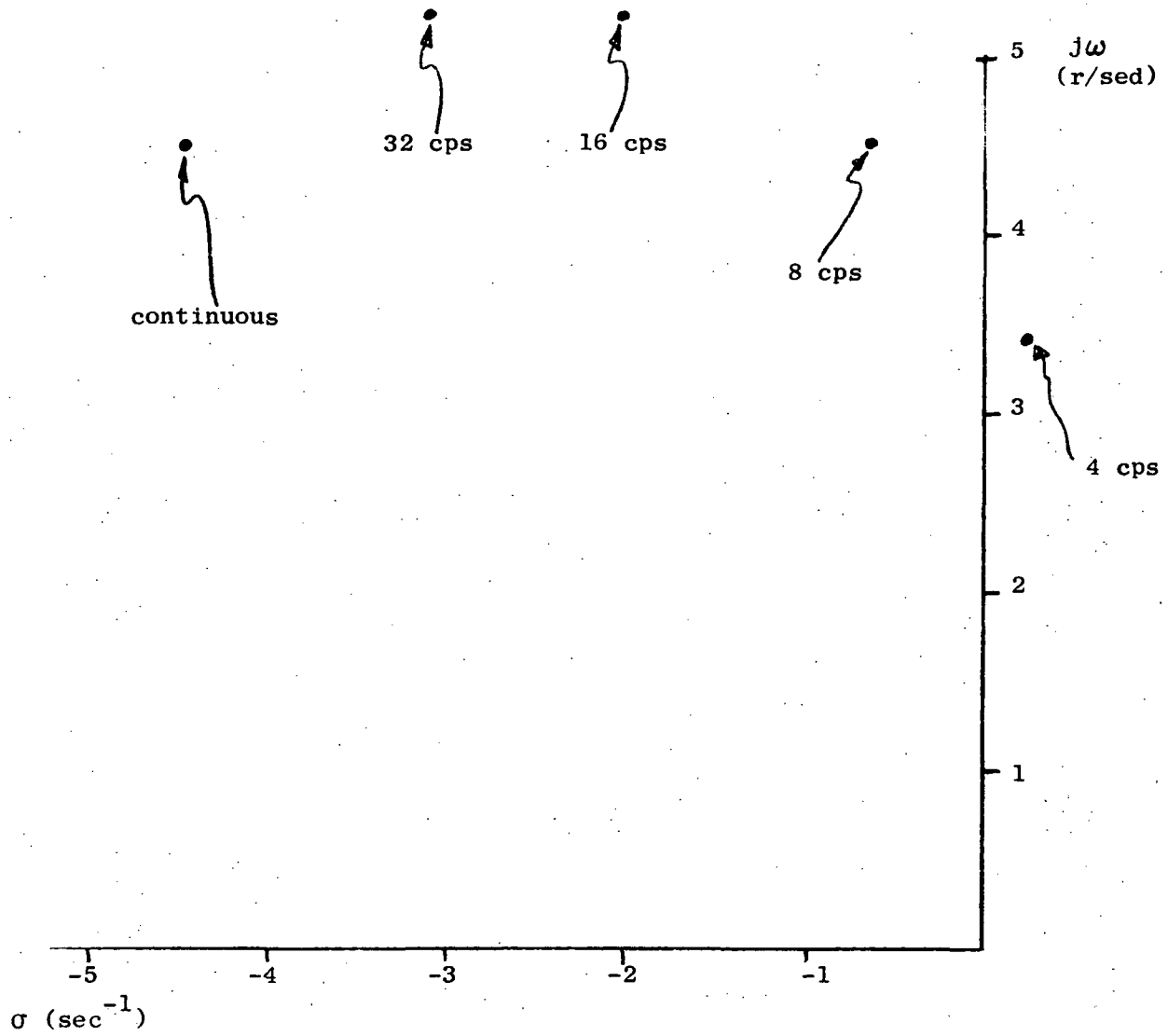
elevator command

Figure 6 Autoland Controller
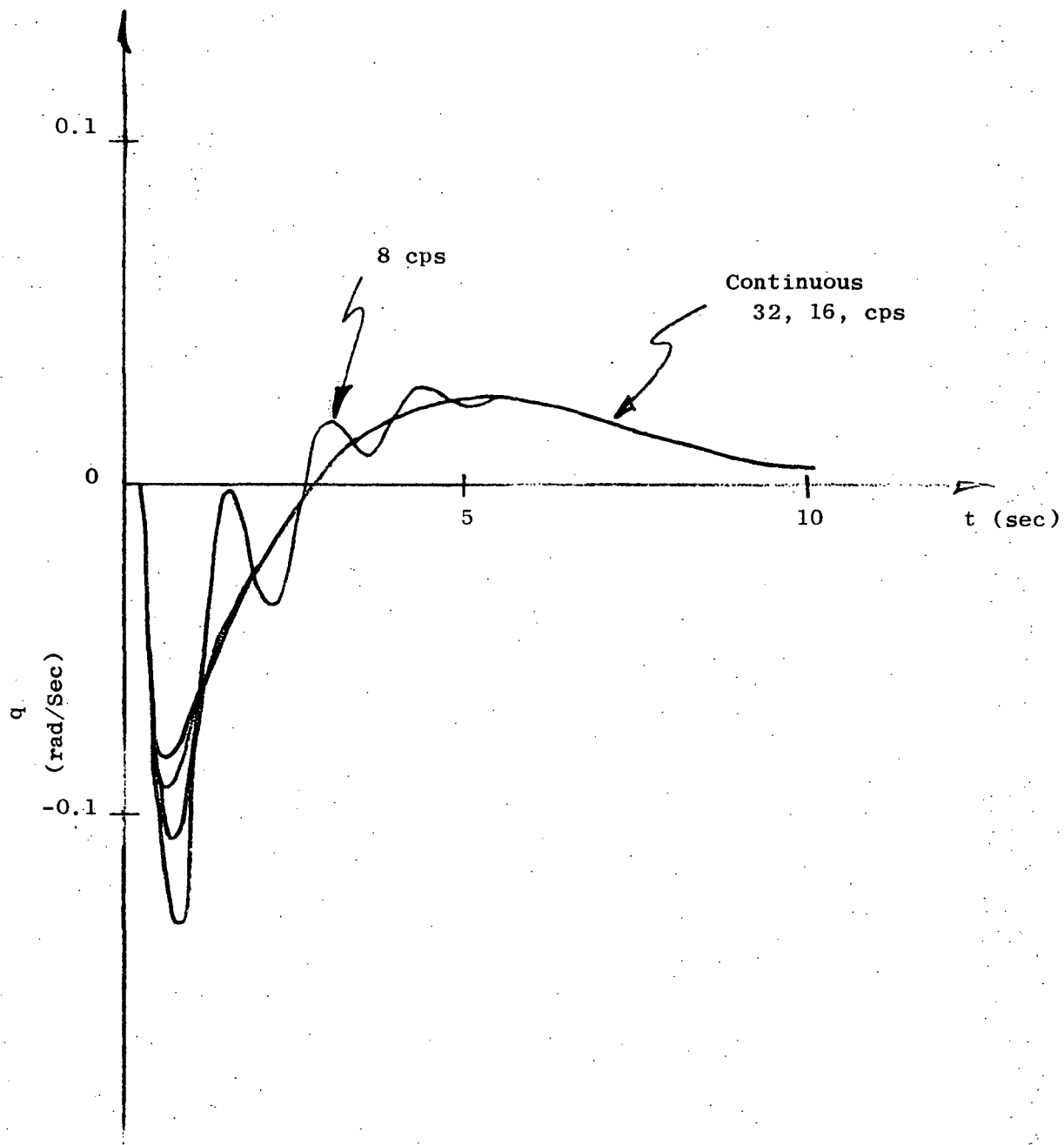
Figure 7 Dominant autoland root locations

Figure 8 Pitch Rate, Autoland

2.3   Digitized S-Plane Design with Hold Approximations

A modification to the design method described in section 2.2 is to include the effect of the ZOH in the s-plane design.   Since this effect is sample rate dependent, the s-plane design needs to be refined for any selected sample rate.   This design technique will be evaluated for the Pitch SAS system which was discussed previously in section 2.2.1.   In this case the s-plane model is represented as shown in Figure 9, where $G_c(s)$ is nominally 1 for the continuous or extremely fast sampling case and varied to cause an acceptable design as T increases.

Assuming that the loss of damping shown to occur in Figure 2 is due primarily to the hold characteristics, some compensation such as a classical lead:

$$H(s) = K_q \frac{(s + A(T))}{(s + B(T))} \quad (A < B)$$

will be required to retain sufficient damping when T increases.   The lead parameters can be chosen to meet root location or frequency response criteria, both of which will be described.
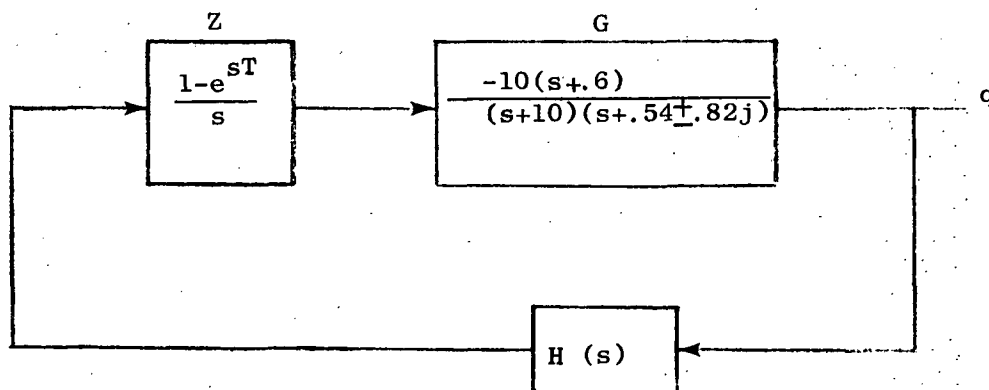

Figure 9   Modified s-Plane Design Model

2.3.1 Root Location Design

If the natural frequency and damping of the short period roots are preserved, the time response will be essentially unchanged. For purposes of constructing s-plane root loci, we approximate the transcendental Laplace transform of the zero-order hold by a rational expression of polynomials in s. Padé approximates,

$$\frac{a_m(-sT)^m + a_{m-1} (-sT)^{m-1} + ---- + a_o}{a_n(-sT)^n + -----a_o} \quad ,$$

of e^{-sT} are formed by matching the largest possible number of terms of the respective McLaurin series by suitable choice of the a_i's and b_i's. The approximates thus formed are given in Table III (from ref. [17]).

	$m = 0$	$m = 1$	$m = 2$
$n = 0$	$\dfrac{1}{1}$	$\dfrac{1 + x}{1}$	$\dfrac{1 + x + \frac{1}{2}x^2}{1}$
$n = 1$	$\dfrac{1}{1 - x}$	$\dfrac{1 + \frac{1}{2}x}{1 - \frac{1}{2}x}$	$\dfrac{1 + \frac{2}{3}x + \frac{1}{6}x^2}{1 - \frac{1}{3}x}$
$n = 2$	$\dfrac{1}{1 - x - \frac{x^2}{2!}}$	$\dfrac{1 + \frac{1}{3}x}{1 - \frac{2}{3}x + \frac{1}{6}x^2}$	$\dfrac{1 + \frac{1}{2}x + \frac{1}{12}x^2}{1 - \frac{1}{2}x + \frac{1}{12}x^2}$

TABLE III - PADÉ Table for e^x (from [17])

The success of the approximation depends on selecting a high enough order of approximate to match the frequency response of the zero-order hold over the bandwidth of interest. Using Table III, we find that the exact hold transfer function,

$$H(s) = \frac{1 - e^{-sT}}{s}$$

reduces to:

$$H(s) \cong \frac{T}{1 + \frac{sT}{2}} \qquad \text{(for n,m = 1)}$$

and

$$H(s) \cong \frac{T}{1 + \frac{sT}{2} + \frac{(sT)^2}{12!}} \qquad \text{(for n,m = 2)}$$

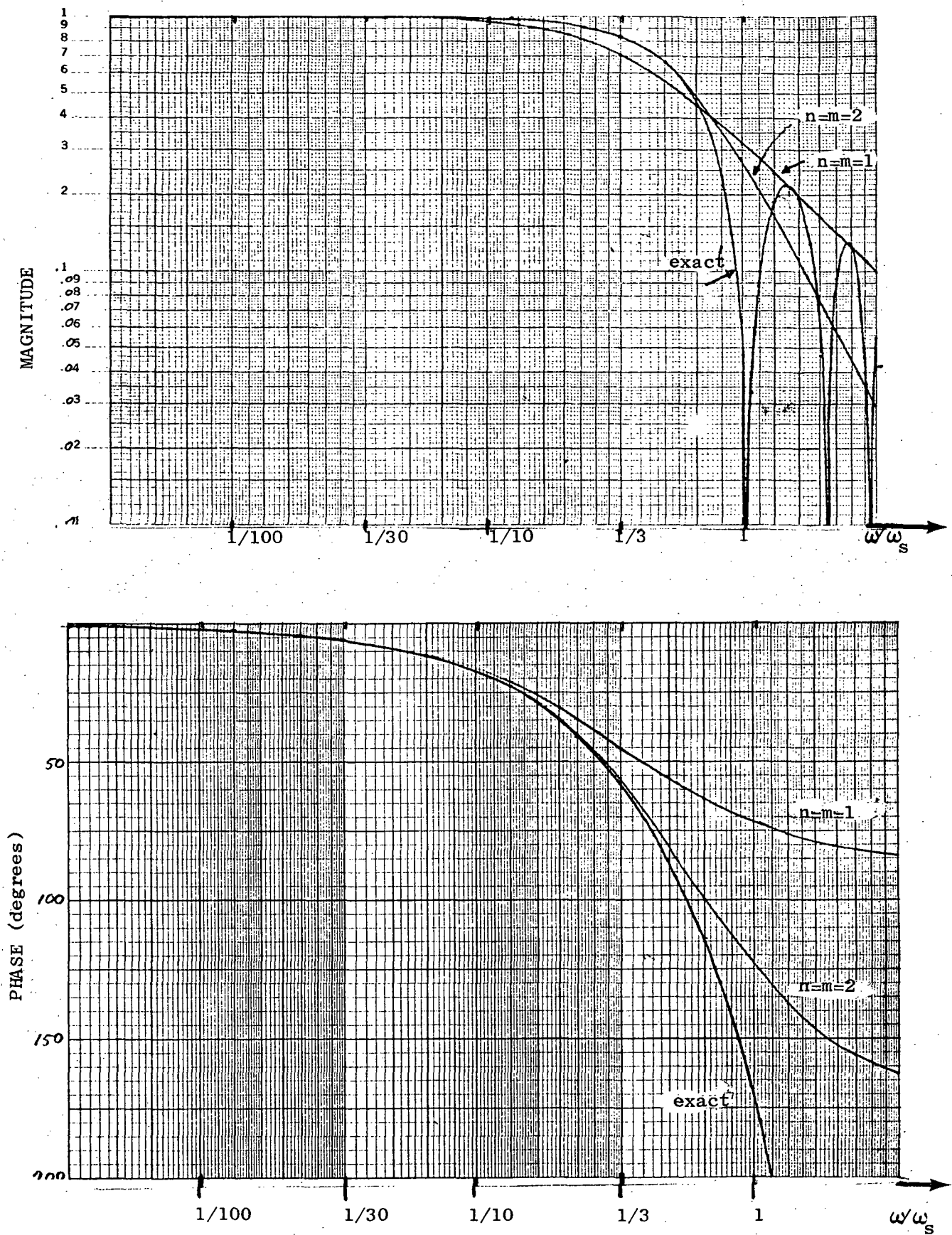Fig. 10 compares the amplitude and phase of all three representations of H(s)

-18-

Figure 10   Frequency Response Comparisons of the Hold
and its Approximations.

The m=n=1 approximate is accurate for frequencies less than 1/10 the sample rate and the m=n=2 approximate is very good for ω less than 1/3 the sample rate. For the short period closed loop poles at approximately 1 cps (Fig. 2), the 2nd order (m,n=2) approximate must be used to evaluate sample rates of 5 cps.

The compensation is designed by arbitrarily locating the lead zero at s=-8 and by successive trials determining the gain K_q and pole location -B which restore the short period roots that have been perturbed by sampling. This is easily done since the transcendental nature of the lag is eliminated by replacing it by a Padé approximate. The results of these calculations are contained in Table IV.

T(sec.)	Kq	A	B
.05	4.15	8	8.85
.1	4.1	8	10.
.2	4.7	8	14.1

TABLE IV - Compensation Parameters

Figure 11 shows the equivalent s-plane roots that result after converting the s-plane design in Table IV to discrete form using Tustin's (or Bilinear) approximation and the matched z-transform.

The Tustin transform is formed by substituting $\frac{2}{T} \frac{z-1}{z+1}$ for s.

$$Kq \frac{s+A}{s+B} \longrightarrow Kq \frac{(AT/2 + 1)}{(BT/2 + 1)} \bullet \frac{z + \dfrac{AT/2 - 1}{AT/2 + 1}}{z + \dfrac{BT/2 - 1}{BT/2 + 1}}$$

The matched z-transform was defined in the previous section. As also described in the previous section, the equivalent s-plane roots are obtained by performing an exact discrete analysis of the system and transforming the z-plane closed loop roots back into the s-plane by:

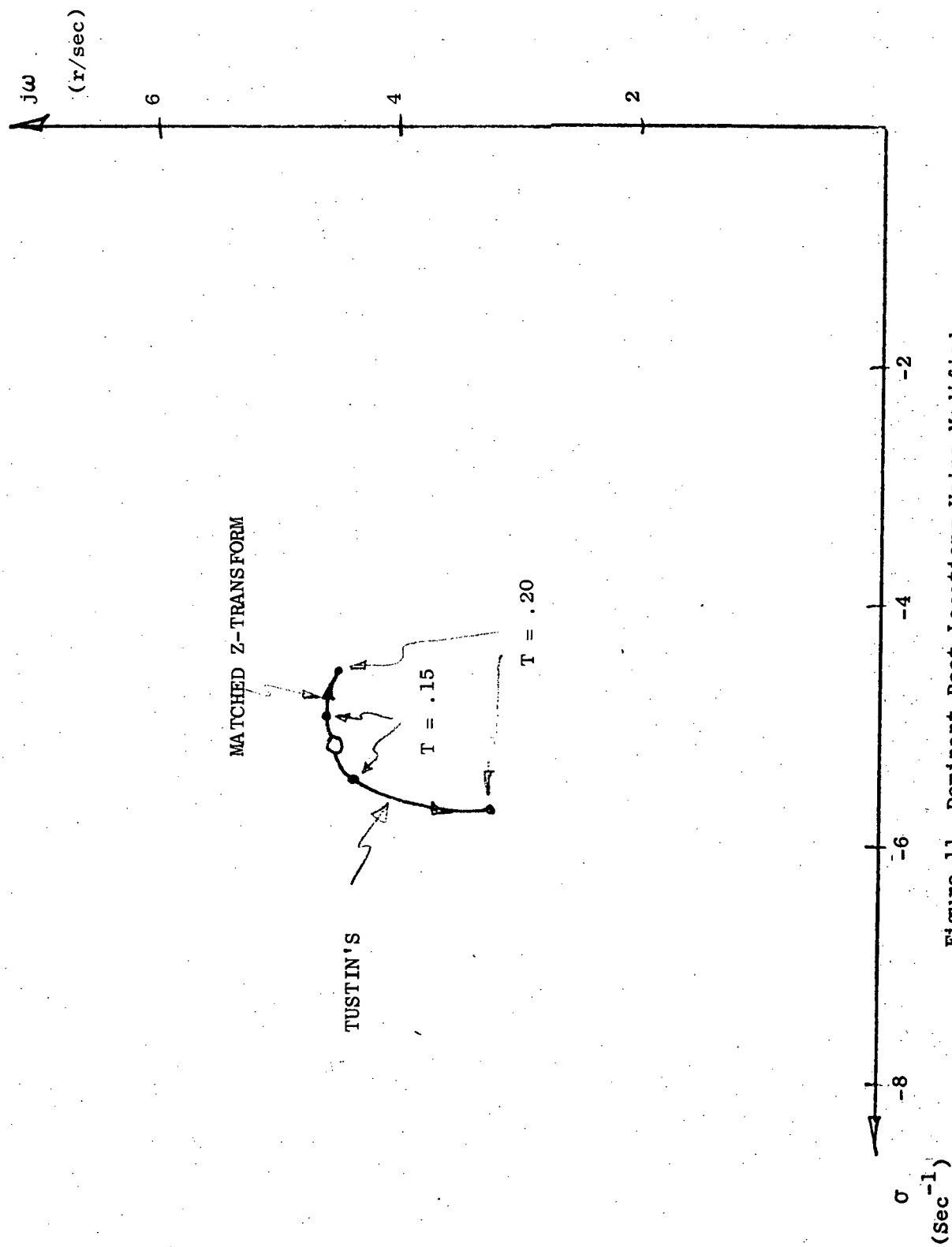$$s = \frac{1}{T} \ell n \, z$$

Figure 11 Dominant Root Locations Using Modified

S-Plane Design

The root migration in Figure 11 is caused primarily by the approximations in the matched z transform and Tustin digitization. The figure shows that root migration at the lower sample rates is much reduced compared to the identical design (Figure 2) performed without the Padé approximate for the hold.

As a further aid in evaluating these designs, frequency response data are presented in Figures 12 and 13 for the Tustin digitization. The open loop gain = 1 crossover frequency can be seen to be lower in the compensated discrete case (GHZ) at ω_s = 5Hz than the continuous case (G). Furthermore, the closed loop bandwidth can be seen in Figure 13 to decrease as the sample rate decreases. These effects occur in spite of the fact that the short period root locations remain essentially unchanged; primarily because the additional root introduced by the compensation affects the frequency response.

2.3.2 Frequency Response Design

An alternate method of choosing the lead compensation is to maintain certain characteristics of the open loop frequency response. In other words, use the lead to restore the frequency response degradation due to sampling.

The closed loop transfer function of plant G with feedback compensation H is:

$$\frac{GZ}{1 + GHZ}$$

where the zero-order hold (Z) must be included for sampled systems.

At low frequency the ZOH and lead network have vanishingly small effect, and the closed loop transfer function is $\frac{G}{1+G}$ as desired. At high frequency where $|GHZ| \ll 1$ the transfer function is GZ instead of G, and the compensation H cannot counteract the zero order hold. But this is well above the bandwidth of the system, the highest frequency of interest. The critical location and sharpness of the Band edge, (Closed loop magnitude of -3db) is heavily dependent on the frequency at which $|GHZ|$ = 0 db and the corresponding phase angle.

ω (rad./sec.)

Magnitude

Z

H

G

GHZ

Block diagram labels: δ_{ec}, Z, G, H, q

Z block: $\dfrac{1-e^{st}}{s}$

G block: $\dfrac{-.10}{s+10}\dfrac{s+.6}{s+54\mp.82j}$

H block: $K_q\dfrac{s+A}{s+B}$
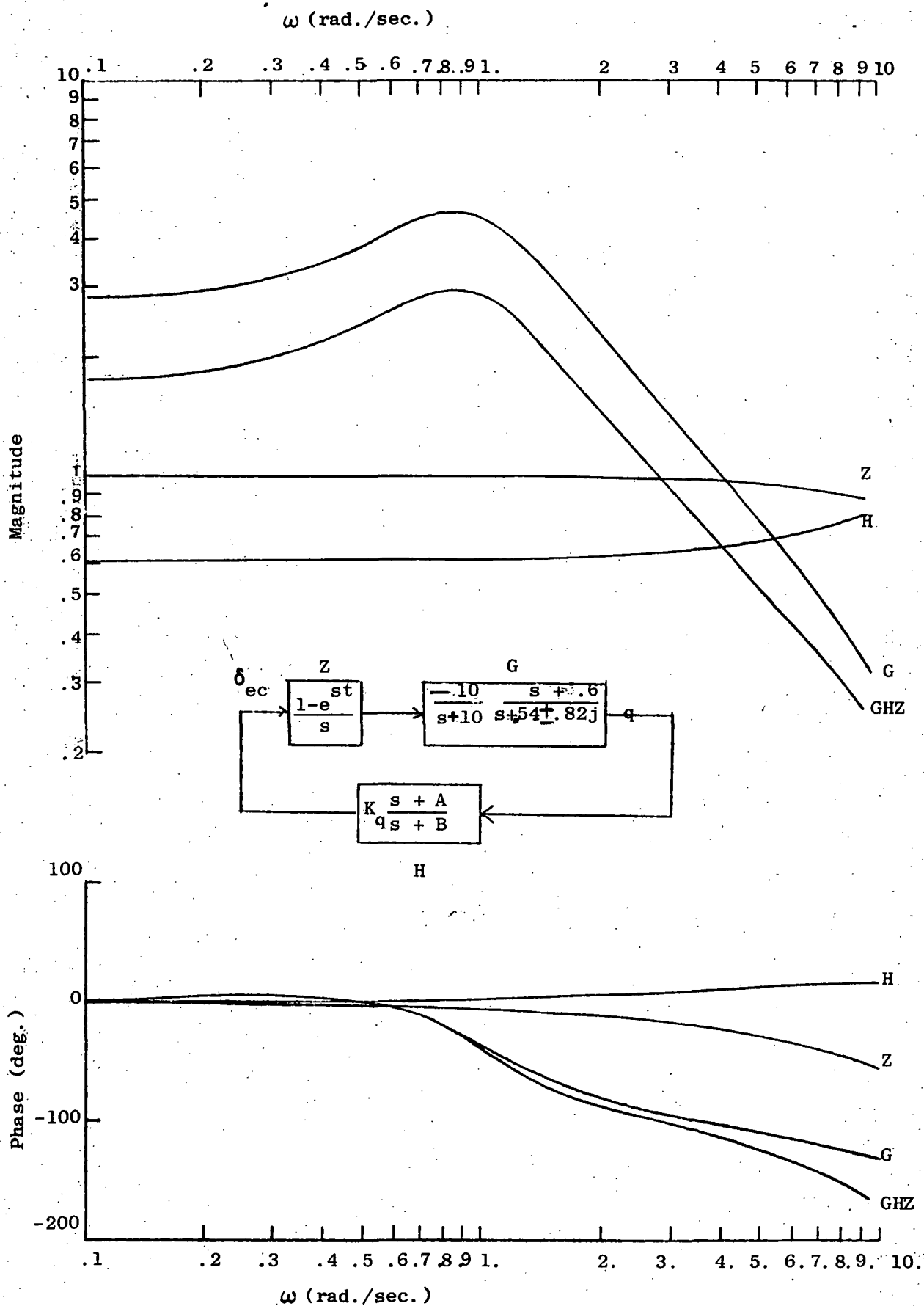
Phase (deg.)

H

Z

G

GHZ

ω (rad./sec.)

Figure 12 Open Loop Frequency Response, s-plane
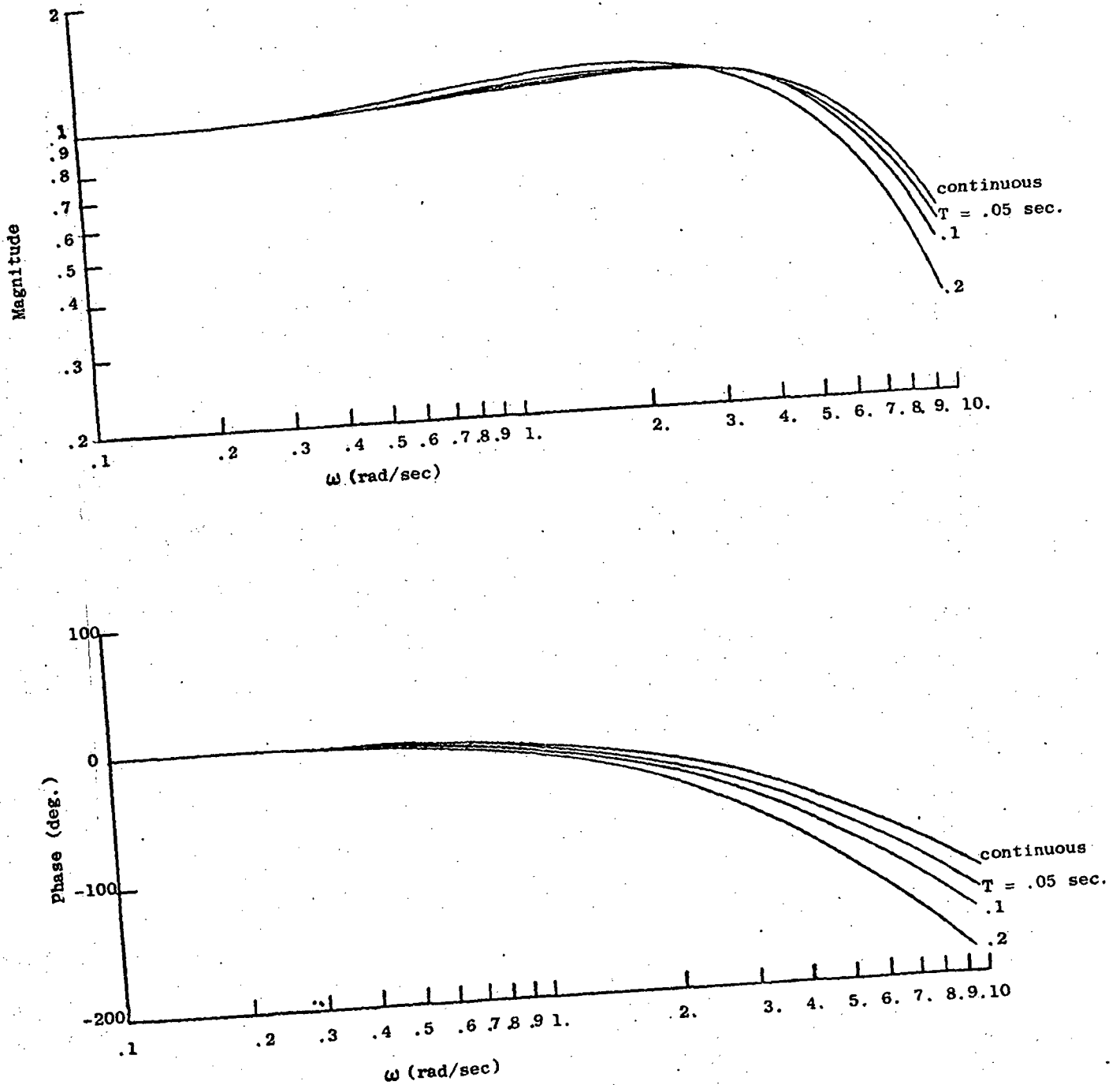
Design, T = .2 Seconds

-23-

Figure 13 S-Plane Design Closed Loop Frequency
Response

-24-

Thus in the frequency response design, $H(s) = K_q \dfrac{s + A}{s + B}$
is picked so that the 0 db or cross-over frequency and phase margin
of G is maintained for GHZ as shown in Figure 14 for 5 cps.

The lead compensation is designed by arbitrarily locating
the zero at $s = -8 \sec^{-1}$ and choosing K_q, and B to meet the phase margin
and gain criterion of 0 db at $\omega = 4.1$ radians/second, the cross-over
frequency of the continuous plant. The parameters thus obtained are
contained in Table V.

<div align="center">

Table V

Lead Compensation by

Frequency Response Design

</div>

T. (Sec.)	K_q	A	B
.01	4.48	8	8.42
.02	4.68	8	8.88
.05	5.41	8	10.54
.1	7.44	8	14.90
.2	31.8	8	64.53

In Figure 15 the equivalent s-plane poles of the discrete system
using the compensation of Table V are shown.

The approximate discrete compensation is formed using both
Tustin (or bilinear) and matched z-transform methods giving rise to two
different s-plane loci.

Also shown in the figure are the s-plane root locations before
digitization. The root movement for the higher order Padé approximates
is due to the preservation of frequency response characteristics.

Furthermore, comparison of the various s-plane designs with
different Padé approximates indicates that the 2nd order Padé yields
sufficient accuracy for this design although for the higher bandwidth
roots at T = .2 seconds there is a noticeable difference between the
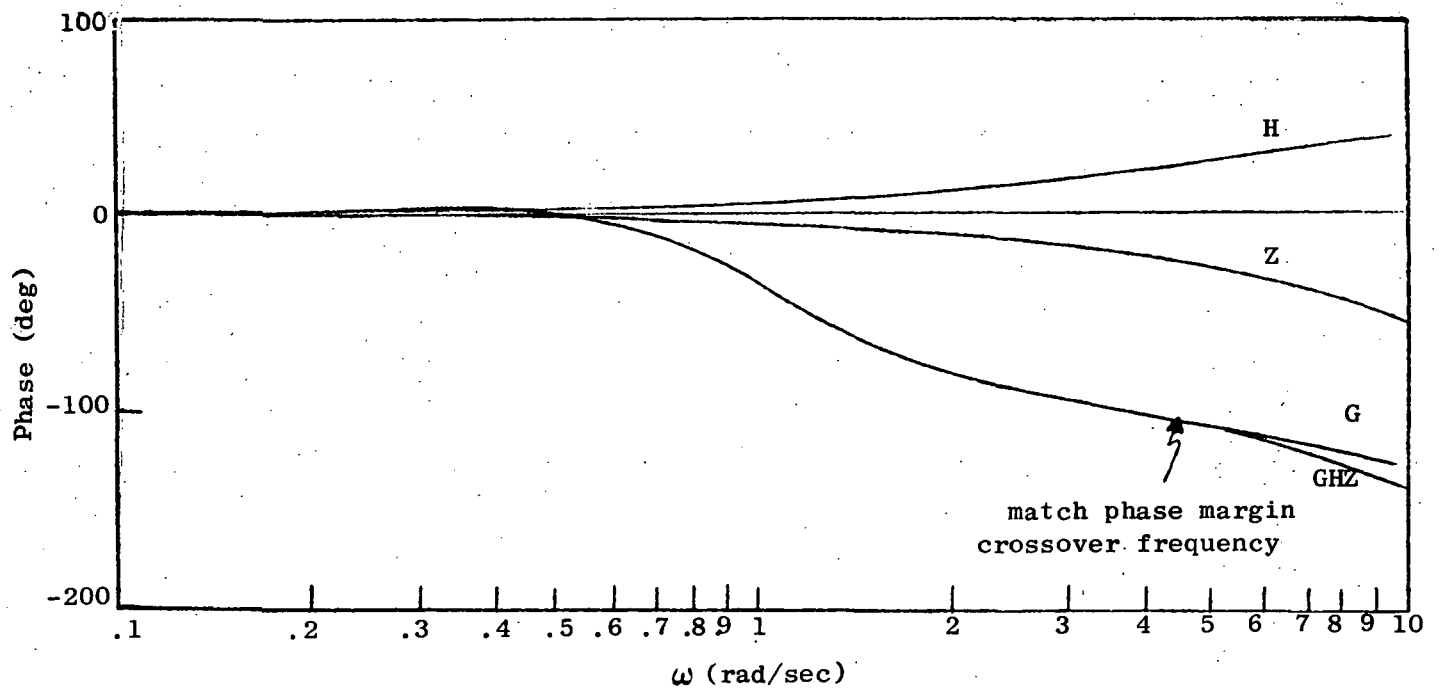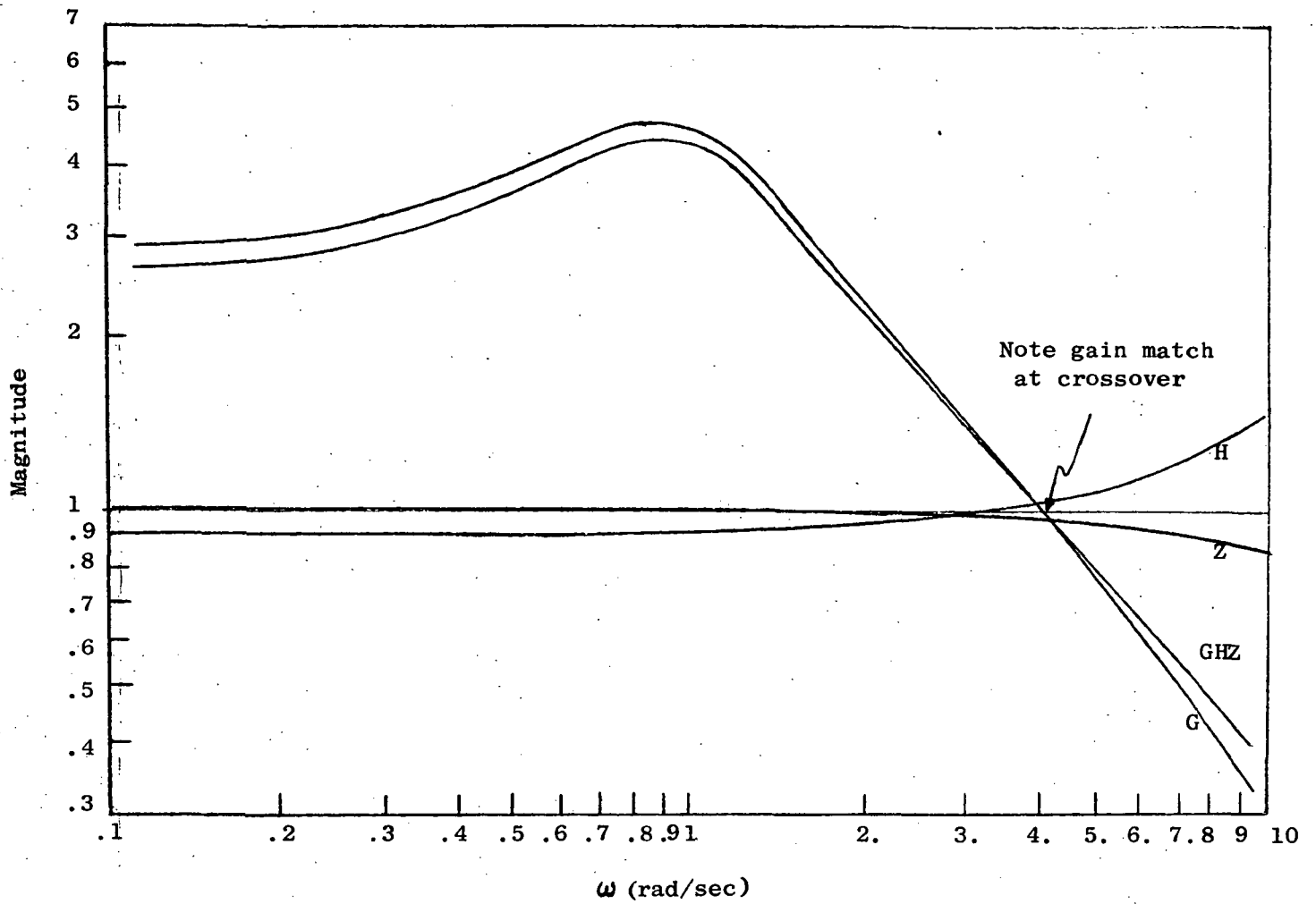2nd and 3rd approximates.

Figure 14   Open Loop Frequency Response,
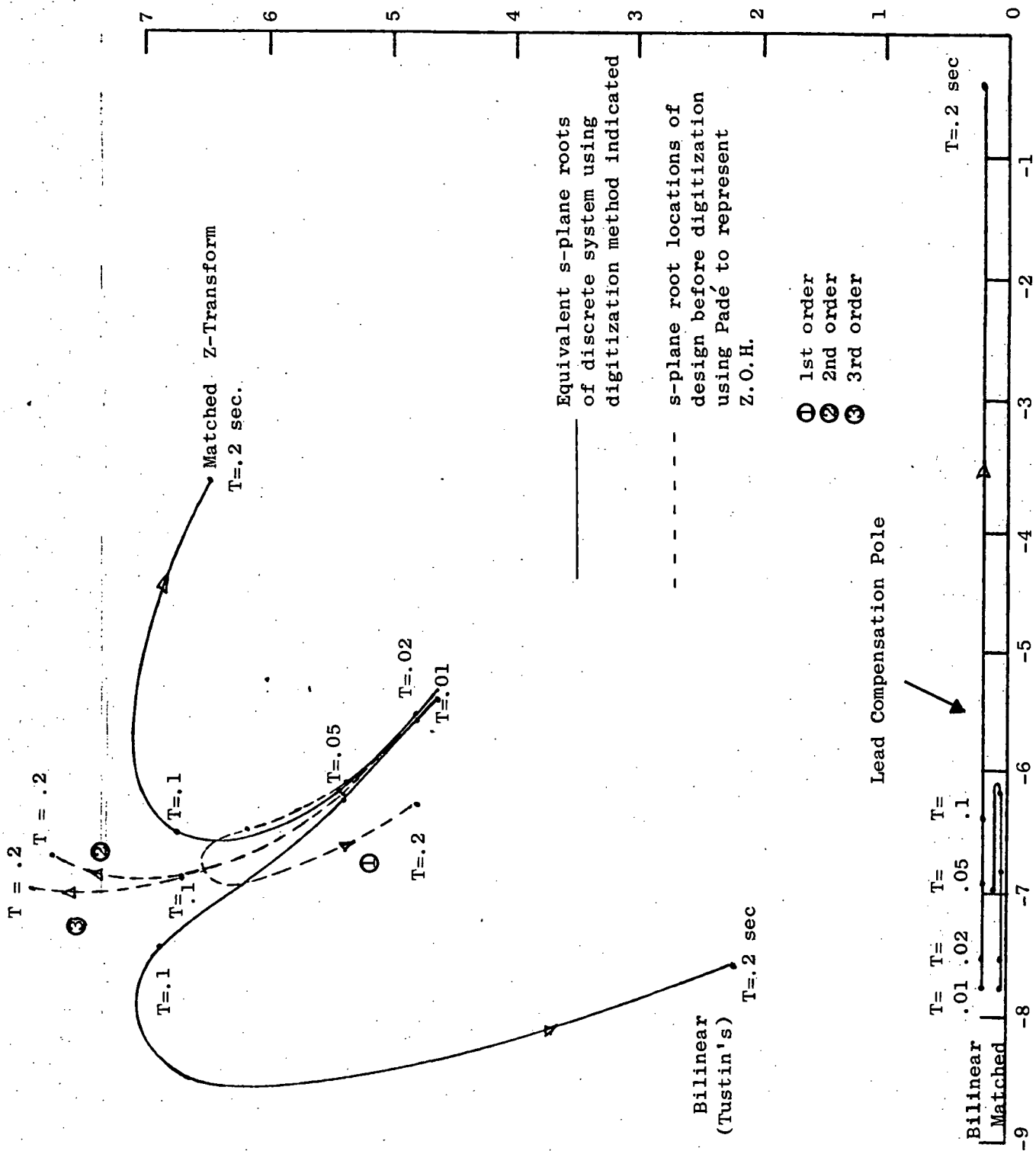
Frequency Response Design (T = .2 sec)

Figure 15 Modified s-plane Design (Frequency Response)

The discretization changes the predicted s-plane roots significantly, especially if the compensation is fast relative to the sample rate. For our case where A = 8, the Bilinear transform is unacceptably inaccurate at moderate sample rates. The z-transform is somewhat more accurate and should be used. The bilinear and matched z-transform and Padé approximate curves coalesce for higher sampling and slower compensation. An example of this is Figure 16 which resulted from a design using the same frequency response techniques but fixing the pole at -9.5 sec^{-1} and varying the zero for proper compensation. The compensation is relatively slow, but clearly the curves are more consistent in this case. However, if the lead compensation pole is too slow, closed loop frequency response will be adversely affected.

The migration of the short period root that occurs in this design (Figure 16) does not adversely affect the closed loop response because the resonant peak from the reduction in damping of the short period is offset by the lag from the real root originating from the compensation pole and zero. Furthermore, the adverse phase lag of the zero-order hold is counteracted by the increased bandwidth of the short period poles.

The closed loop frequency response characteristics of the designs with lead parameters given in Table V and root locations given in Figure 15 are shown in Figure 17. Comparing these results to the designs based on short period pole fixing (Figure 13), we find that the magnitude matches better at low frequencies and the phase is slightly better over all frequencies.

The designs with slower compensation yielded less discretization errors (note correspondence between dotted curves and solid curves in Figure 16) because of the slower compensation to be digitized; however, the slower compensation yielded a poorer match to the continuous system at the lower frequencies than either the fast compensation frequency response design on the root location design.

Either frequency response design criteria or dominant root location design criteria appear to be feasible methods for adjusting

-28-
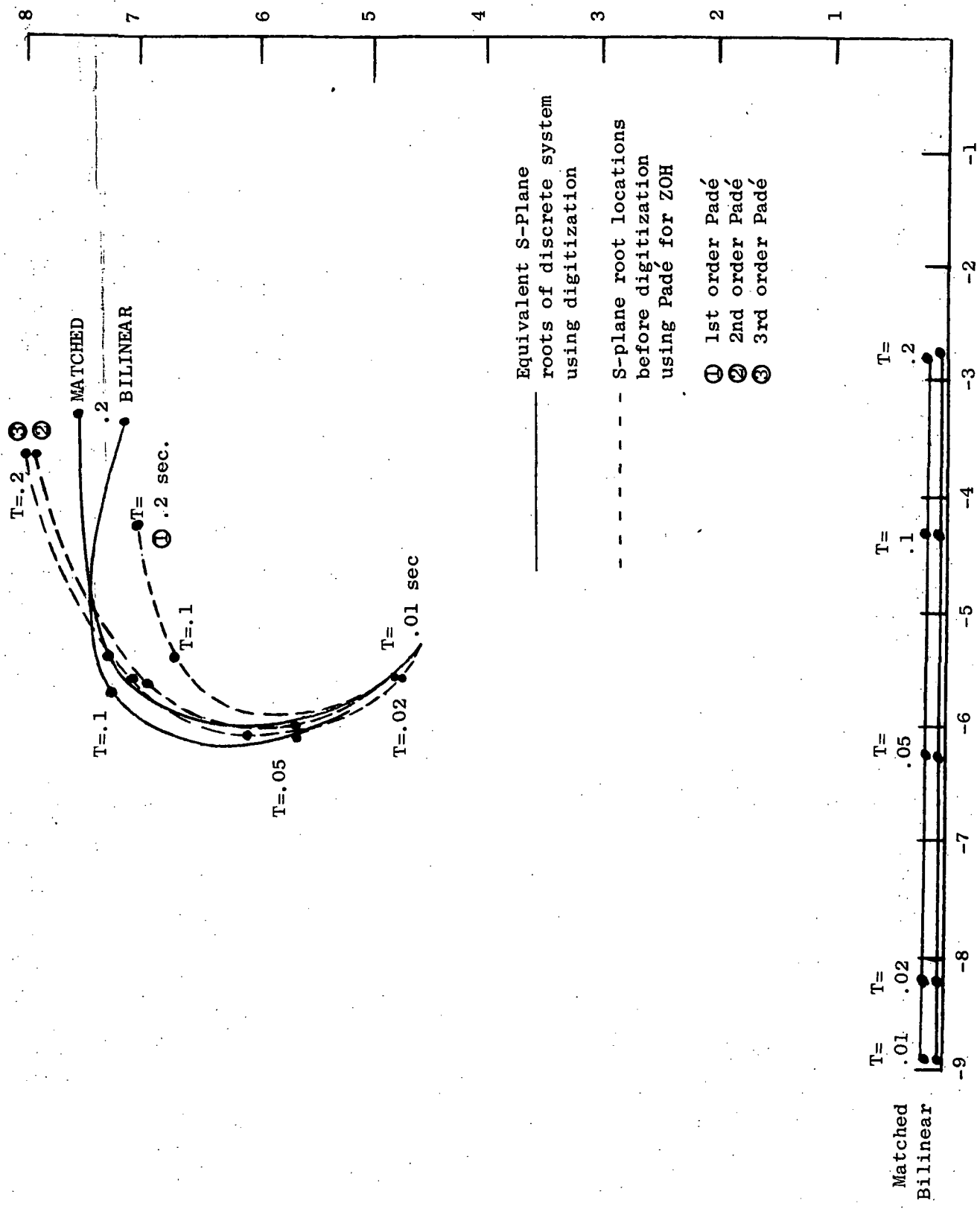
Figure 16 Modified S-Plane Design (Freq. Response)
slow compensation
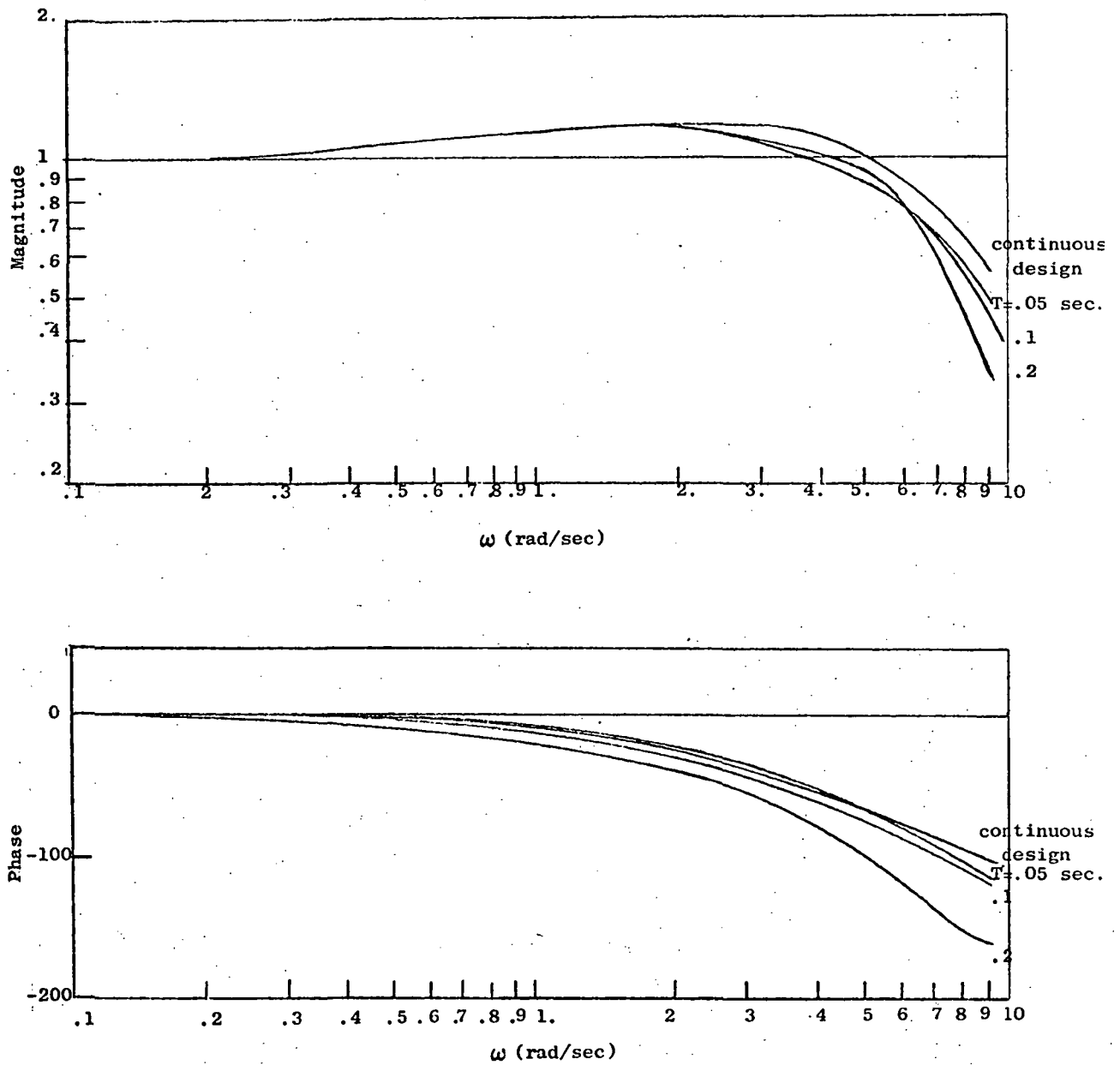
Figure 17 Closed Loop Frequency Response

For Frequency Domain Design (T = .2 seconds)

the s-plane designs for the effect of sampling in the cases studied. The frequency response method, however, appears to offer a more reliable method in general since movement of all roots is accounted for in the design criteria. For flight control modes with higher order dynamics, it may be more difficult to pick the dominant poles and adjust the compensation without introducing some new dominant pole.

2.4 Direct Digital Design

Direct digital design refers to the design of a controller in the z-plane (or the w-plane, with an appropriate transformation). It differs from digitized s-plane design in that the effects of the hold circuit are known exactly at all sampling rates. In the z-plane, techniques such as root locus and pole placement may be used exactly as they are in the s-plane.

Direct digital design is most widely used in the construction of estimators or of controllers with state variable feedback inasmuch as optimal control techniques may be applied with little change to the discrete system. However, the starting point for most digital systems is a continuous mechanization, for which engineers still have the most insight as well as an arsenal of design tools. The object, therefore, is not to completely redesign the system, but instead, to have changes to account for the discrete characteristics and the lag of the hold circuit. Toward this aim, two of the systems discussed in the section on digitized s-plane design (2.2) were re-analyzed with the addition of a lead network at the input to the hold circuit. The lead ratio and gain of this network was chosen in order to place the dominant poles of the closed-loop system at the location chosen in the continuous design. This process can, in general, be done by trial and error; but for this effort, a systematic procedure was developed and implemented in a computer program (called LEAD, See Appendix A). It calculates the lead required from the pole/zero constellation in the z-plane. It is important to note that this design was performed in the z-plane, which is an exact representation of the digital system. This FORTRAN computer program has been expanded so that it contains options to do the analysis of the s-plane design method as well as calculating the lead network.

2.4.1 Pitch SAS

To the SAS system shown in Figure 1 is added a digital lead network which performs the equivalent of the continuous lead:

$$K \cdot \frac{\tau_1 s + 1}{\tau_2 s + 1}$$

using the matched z-transform method, the digitized version of this becomes:

$$\frac{f(z)}{e(z)} = K \bullet \frac{1 - e^{(-T/\tau_2)}}{1 - e^{(-T/\tau_1)}} \bullet \frac{z - e^{(-T/\tau_1)}}{z - e^{(-T/\tau_2)}}$$

The constants for this lead network were determined so as to match the equivalent s-plane complex roots of the discrete system with the original complex roots at $s = -5.15 \pm 4.5j$. Table VI shows the lead network characteristics determined and the resulting equivalent s-plane root locations. Except for the 4 cps case, the complex roots were matched exactly while the position of the additional real root added by the network varied. The inability to match precisely the 4 cps complex

TABLE VI

Pitch SAS Lead Characteristics

Sampling Rate	$1/\tau_1$	$1/\tau_2$	K	Roots
32 cps	8.0	8.46	0.917	-0.77, -5.15 ± 4.5, -7.75
16	8.0	9.03	0.841	-0.79, -5.15 ± 4.5, -7.45
8	8.0	10.7	0.714	-0.82, -5.15 ± 4.5, -6.75
4	8.0	75.	0.45	-0.97, -5.14 ± 3.12, -5.08

roots was due to the arbitrary design procedure of fixing the lead zero at 8 r/sec and varying the lead pole to obtain the desired roots. A zero placement closer to the s-plane origin would have allowed matching at 4 cps also.

The additional real root arising from the lead compensation dynamics is sufficiently fast to have a relatively small effect on the system response. However, for progressively slower sampling the root becomes progressively slower and more important in the response. In subsequent designs, the detrimental effects of the additional real root on the transient response will be evaluated.

2.4.2 Pitch Attitude Control-Wheel Steering

Just as for the SAS described above, an appropriate compensation for the control-wheel steering mode is a lead network at the output of the digital controller (see Figure 18). LEAD was used to match the dominant poles at $-1.34 \pm 2.13j$. With decreasing sampling rate, however, one of the faster roots moves toward the origin to influence the system response. Basically, there is no way to keep all the system roots constant with a decreasing sampling rate with only one compensation. However, there is a great improvement in performance i.e. the response is good down to 4 cps, whereas the system with a digitized s-plane design goes unstable. Table VII presents the parameters of the digital lead network employed, and Figure 19 indicates that there is no movement of the root at $-1.34 \pm 2.13j$ at all versus sampling rate. That figure also shows the position of the next faster root at 4 cps versus the lead network zero (sampling faster than 4 cps puts this root on the negative real axis and much faster than the dominant root). Since these two roots have bandwidths of the same order of magnitude, they both must be taken into consideration in determining performance. Figures 20 and 21 show the pitch error and pitch rate transient response for an initial pitch error of 0.1 radian with lead compensation (they may be compared directly to Figure 5). Although there is some degradation in transient performance, it is considerably better than that of the system without compensation.

Figure 18 Control Wheel Steering (Discrete Design)

Table VII
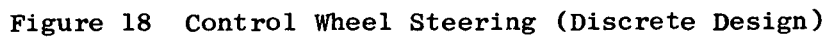
Control Wheel Steering Lead Characteristics

Sampling rate	$1/\tau_1$	$1/\tau_2$	K
32 cps	2.0	2.23	0.87
16	2.0	2.49	0.77
8	2.0	3.31	0.61
4	2.0	6.03	0.45
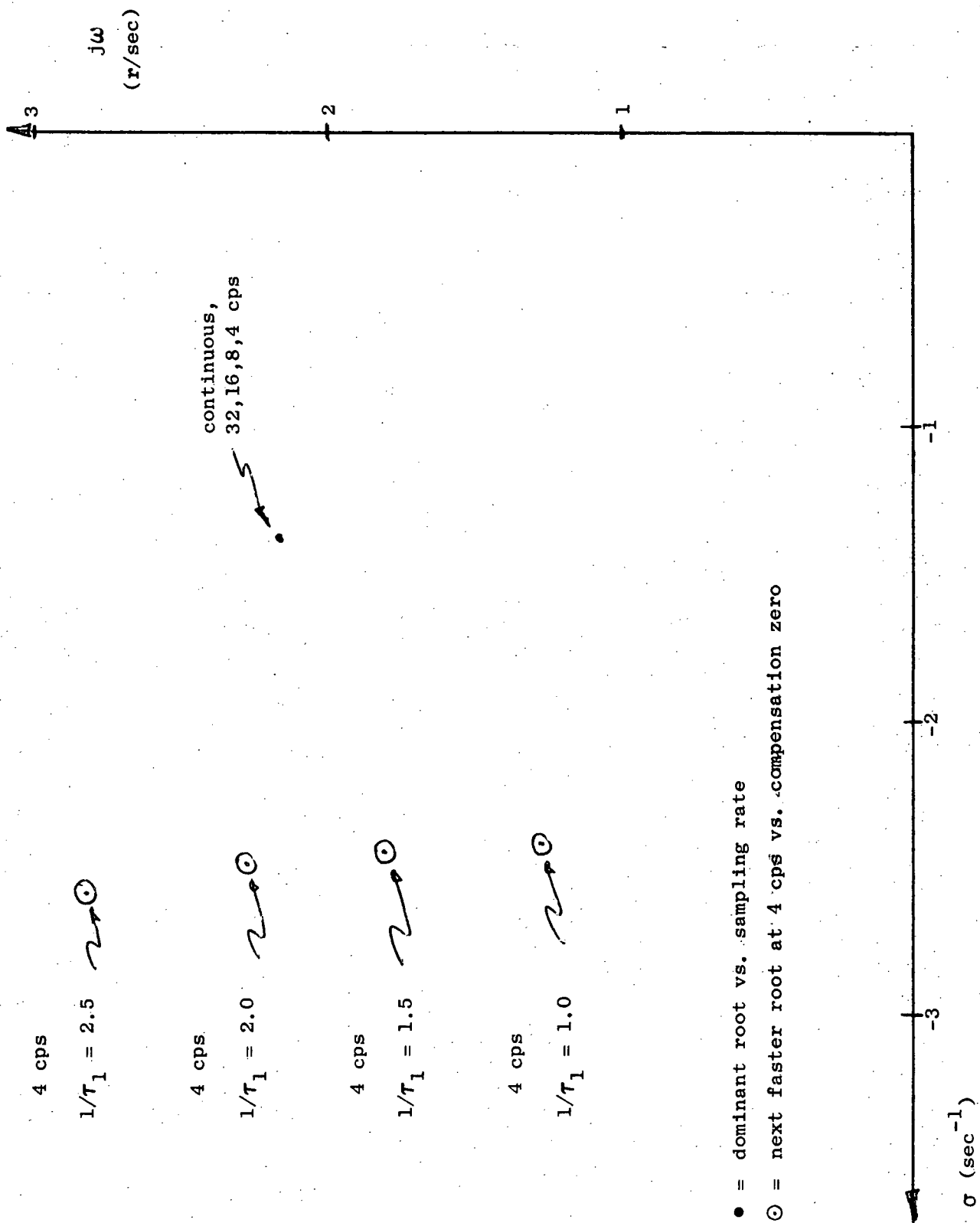
Figure 19 Control Wheel Steering Mode Equivalent S-Plane Roots

• = dominant root vs. sampling rate

⊙ = next faster root at 4 cps vs. compensation zero
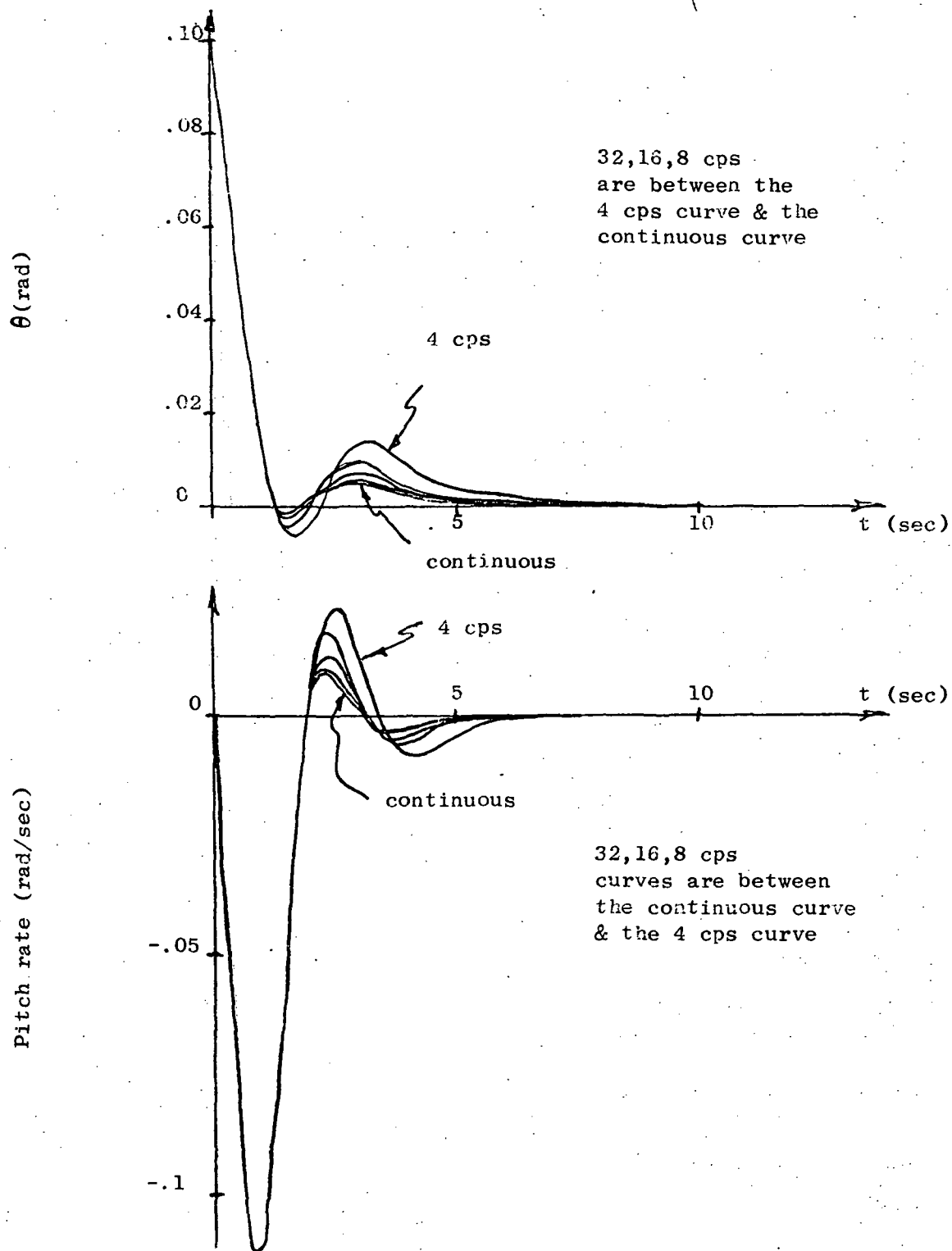
Figure 20   Pitch angle/rate, Control Wheel Steering
(Discrete Design)

2.5 Discrete Design Using Optimal Techniques

An alternate method to the design techniques discussed so far is to use modern control's "optimal" estimator/controller approach. This entails a somewhat arbitrary selection of weighting factors in a cost function; however, once these are selected, the discretization process is routine.

An estimator/controller implementation can be exactly the same as a classical compensator, the difference being solely in the methods used to arrive at the design. In many continuous cases, however, the estimator/controller design results in a higher order compensation than would result using classical methods; for discrete systems, the difference in order is less pronounced.

Design of compensation using modern methods is made up of two parts; the controller and the estimator (sometimes called an observer). The controller is determined by minimizing the quadratic performance index:

$$J_c = \frac{1}{2} \int_0^\infty \left[x^T A x + u^T B u \right] dt$$

and the estimator by minimizing:

$$J_o = \frac{1}{2} \int_0^\infty \left[(z - Hx)^T R^{-1} (z - Hx) + w^T Q^T w \right] dt$$

where

      x is the state vector

      x = estimated state vector

      u = control vector

      z = measurement vector

      H = measurement state distribution matrix

      A = state weighting matrix

      B = control weighting matrix

      W = process noise vector

      Q = white process noise power spectral density matrix

R = white measurement noise power

      spectral density matrix

v = z - Hx = measurement error vector

It can be shown, (ref. [18] [19]) that the solution of the optimal control and estimation problem consists of linear state feedback to the control u and linear measurement error feedback to the estimator:

$$u = C\hat{x}$$
$$\dot{\hat{x}} = (F + GC)\hat{x} + K(z - H\hat{x})$$

Using eigenvector decomposition methods [19], [20] the steady state controller gains, C, and estimator gains, K, can be efficiently determined. To accomplish this, the A, B matrices and the Q, R values of the noise model are chosen to give a "satisfactory" system design. The judgement in determining when the system is satisfactory is based on the same factors that one would use for a classically designed system. In this particular design exercise, the goal is to obtain a modern design which has all the same root locations as the previous design methods; thus enabling a direct comparison with the other methods. Therefore, A, B, Q, and R were selected to yield identical closed loop short period roots while maintaining the additional roots which occur with the introduction of the estimator relatively fast. The bias estimate state (which performs the same function as the classical washout) is an exception to this; its root was maintained at the washout break point.

A continuous controller/estimator for the Pitch SAS with a washout was determined for the TCV vehicle. The state space model for the aircraft was given in section 2.2.1. Combining this with the actuator model and augmenting the state to account for a possible bias in the pitch rate measurement (the equivalent of a washout), we obtain the system model:

$$
\begin{bmatrix} \dot{q}_b \\ \dot{w} \\ \dot{q} \\ \dot{\delta e} \end{bmatrix} = \begin{bmatrix} 0 & 0 & 0 & 0 \\ 0 & -.628 & 207 & -.14 \\ 0 & -3.28^{-3} & -.45 & -1.74^{-2} \\ 0 & 0 & 0 & -10. \end{bmatrix}^{\dagger} \begin{bmatrix} q_b \\ w \\ q \\ \delta e \end{bmatrix} + \begin{bmatrix} 0 \\ 0 \\ 0 \\ 10 \end{bmatrix} \delta e_c
$$

$$y = Hx + v$$

where:

$H = [1010]$;

q_b = pitch rate measurement bias

q = pitch rate

w = z-component of aircraft velocity

δ_e = elevator angle in degress

δ_{e_c} = commanded elevator angle

y = measurement

The values of A and B selected for use in the cost function

were:

$$
A = \begin{bmatrix} 0 & 0 & 0 & 0 \\ 0 & .33 & 0 & 0 \\ 0 & 0 & 7.337^{4} & 0 \\ 0 & 0 & 0 & -.86 \end{bmatrix} \qquad B = 1
$$

which yielded:

$$C = [0, -1.32^{-8}, 247.23, 9.0^{-9}]$$

the values of Q and R selected are:

$$
Q = \begin{bmatrix} 22.877 & 0. & 0. & 0. \\ 0. & 5.03^{8} & 0. & 0. \\ 0. & 0. & 33.92 & 0. \\ 0. & 0. & 0. & 1.106^{7} \end{bmatrix} \qquad R = 1
$$

which yielded:

$$
K = \begin{bmatrix} 4.783 \\ -1.908^{4} \\ 8.816 \\ -314.5 \end{bmatrix}
$$

$\dagger$ the notation 3.1^{-3} means 3.1×10^{-3}

For comparison purposes, the poles and zeros of the resulting design's open loop transfer function were computed . Figure (21) shows the selected closed loop root locations and a root locus vs the open loop gain. This design yields three roots more than a classical design with a washout. If compensating the system using classical methods to overcome effects of sampling, one or two extra roots may be added, a step that is not required when discretizing a controller/estimator design.

By formulating the system equations in a discrete fashion but using an identical cost function and weighting values to the continuous design, an optimal discrete controller/estimator results which closely matches the performance of the continuous design.

In this case, the discrete system representation is as stated in section 2.2 and results in a discrete controller:

$$u_i = C\hat{x}_i$$

$$\hat{x}_{i+1} = \bar{x}_{i+1} + K(z_{i+1} - H\bar{x}_{i+1})$$

$$\bar{x}_{i+1} = \Phi\hat{x}_i + \Gamma u_i$$

$$z_i = Hx_i + v_i$$

or -
$$\hat{x}_{i+1} = \Phi\hat{x}_i + \Gamma u_i + KH\Phi(x_i - \hat{x}_i) + Kv_{i+1}$$

The actual cost function used in the minimization was discrete, i.e.:

Controller:
$$\min_{u_i} J = \frac{1}{2}\sum_{i=0}^{\infty}\left[x_i^T A_D x_i + u_i^T B_D u_i \right]$$

Estimator:
$$\min_{x_i} J = \frac{1}{2}\sum_{i=0}^{\infty}\left[w_i^T Q_D^{-1} w_i + (z_i - H\hat{x}_i)^T R_D (z_i - H\hat{x}_i) \right]$$

however, the values of A_D and B_D are computed [20] based on A and B from the continuous design. The values of Q_D and R_D are the same as the Q and R used in the continuous system optimization. Eigenvector decomposition methods[19,20] yield a very efficient tool in solving for the optimal gains for either the continuous or discrete problem. Figure (22) shows the equivalent s-plane root locations for the discrete system designed as a continuous system in Figure (21). The roots show very little migration due to sampling. Figure (23) shows the closed loop
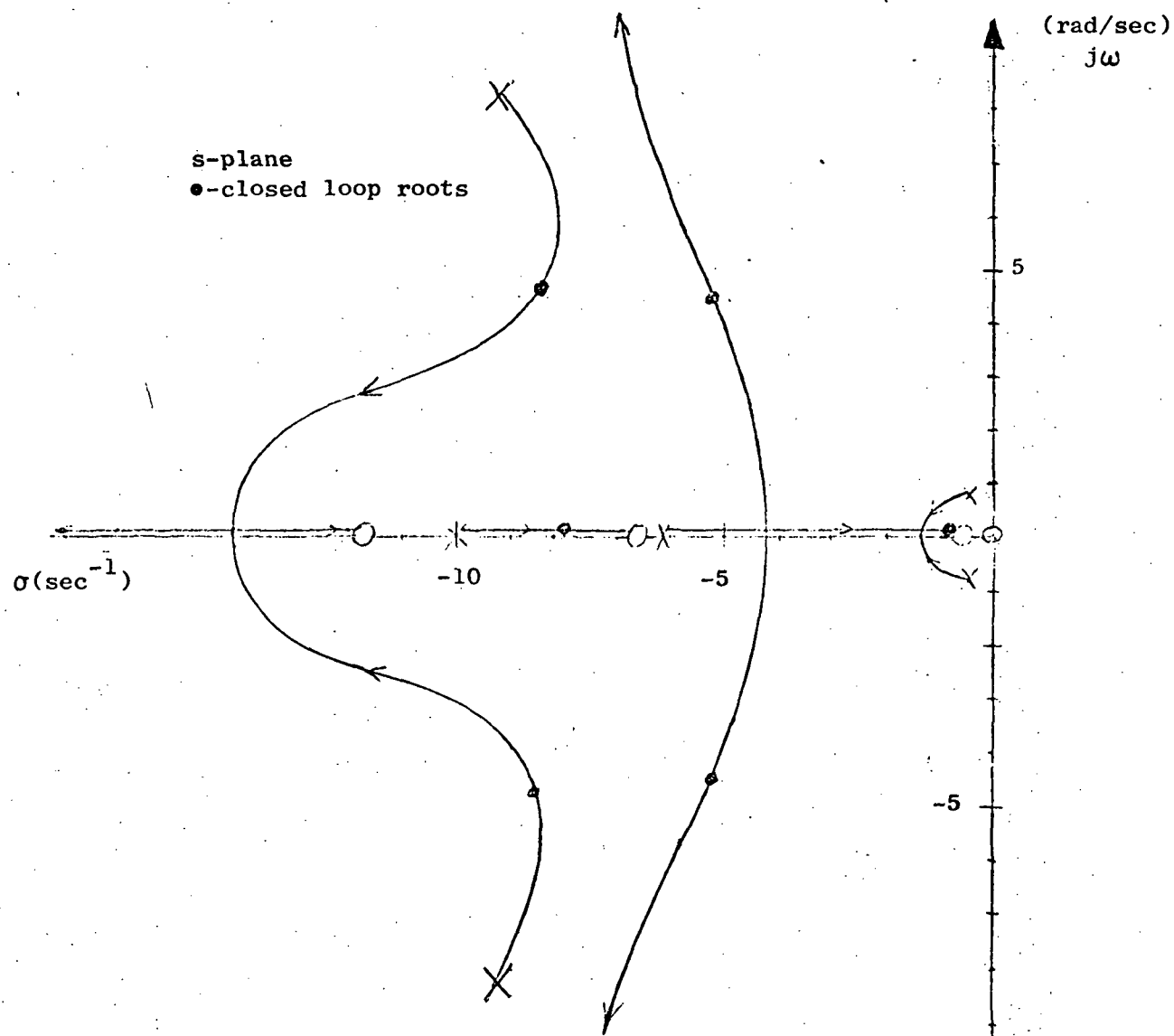
Figure 21   Root Locus vs Open Loop Gain of
Controller/Estimator Design

-42-
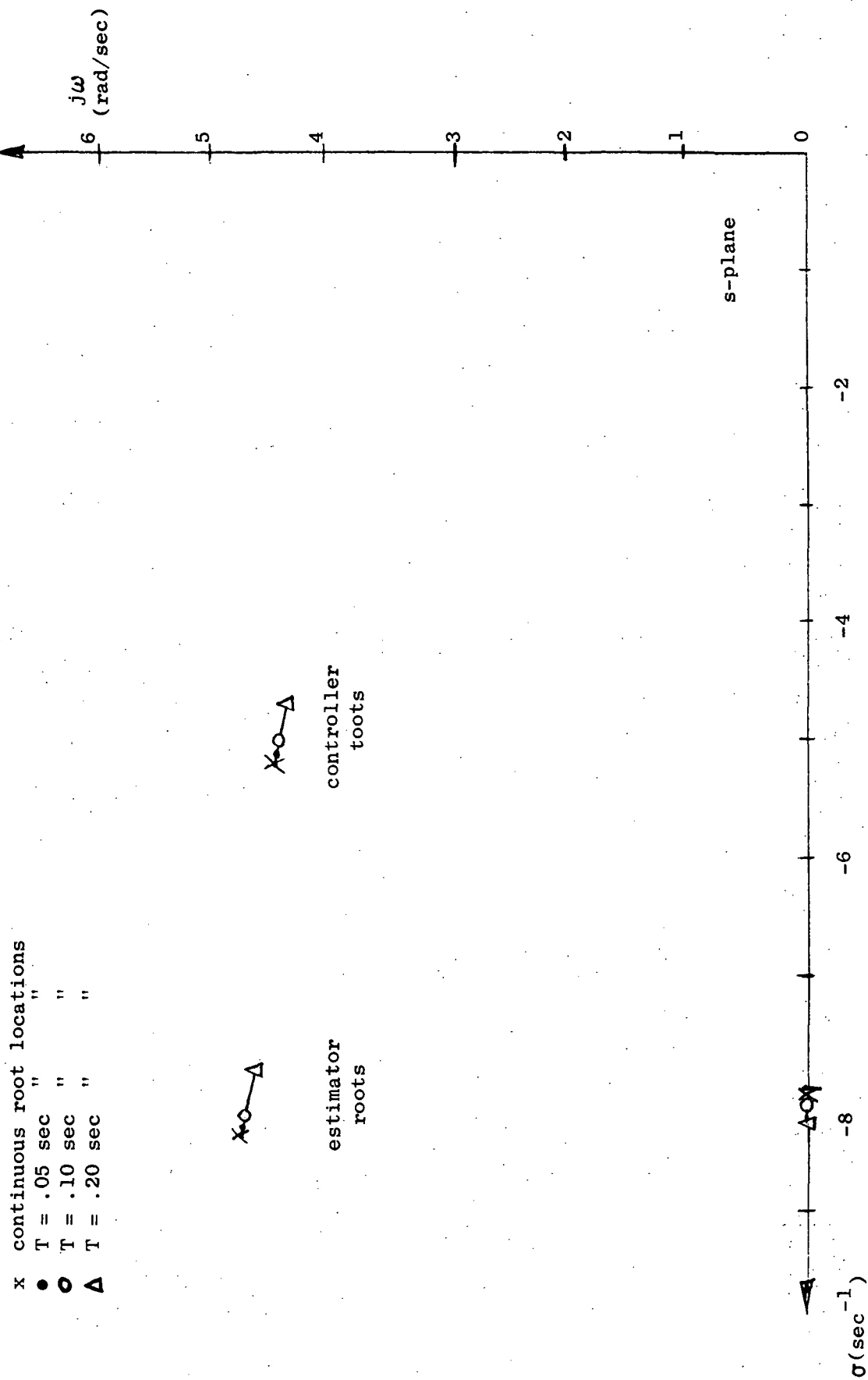
Figure 22   Root Locus of Controller/Estimator Design vs. Sample Period

x   continuous root locations
●   T = .05 sec   "   "
○   T = .10 sec   "   "
△   T = .20 sec

$j\omega$ (rad/sec)

s-plane

controller roots

estimator roots

$\sigma(\text{sec}^{-1})$

-43-

ω (rad/sec)
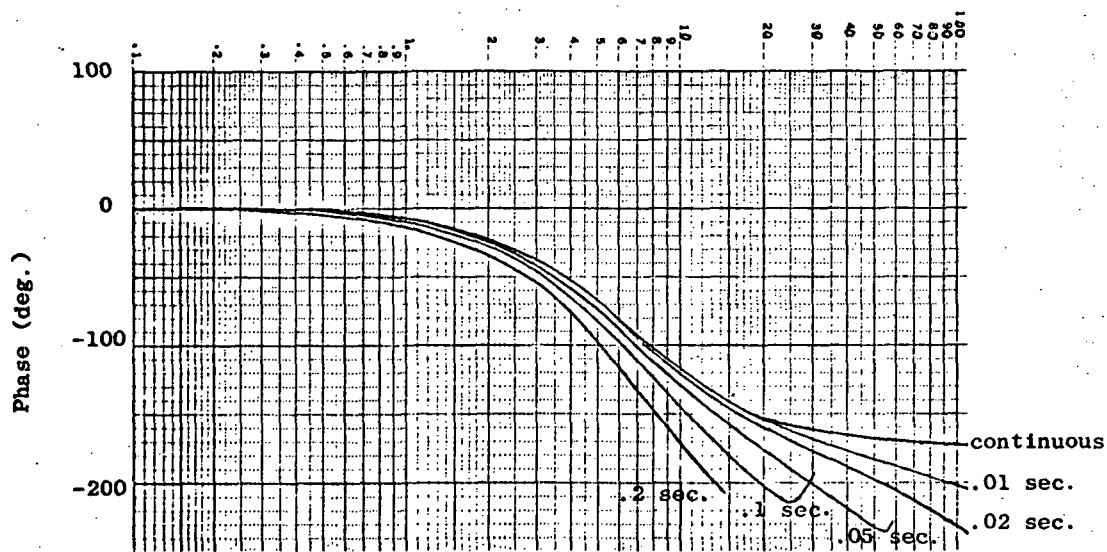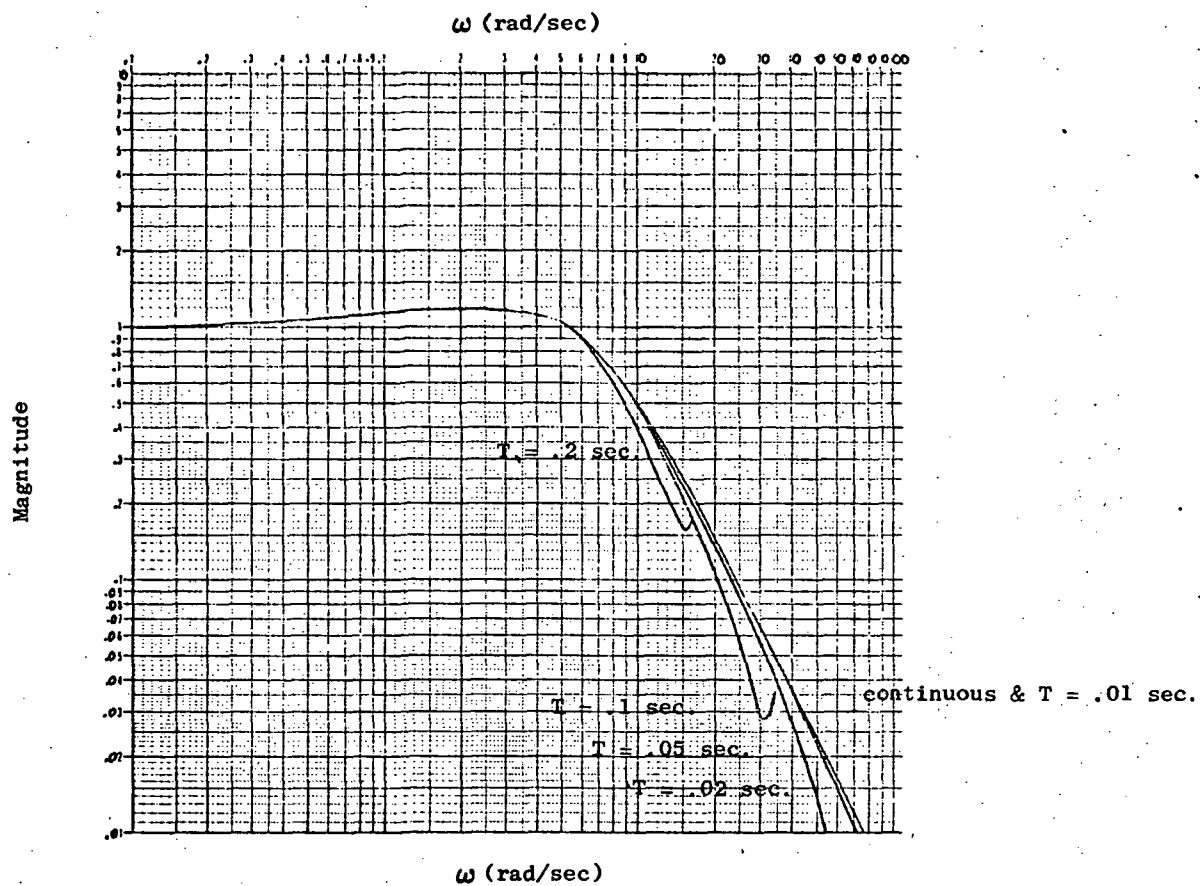
Figure 23 - Closed loop Frequency Response versus
Sample Period for Design Using Quadratic Synthesis

-44-

frequency response characteristics for the various sample rates. To demonstrate the modification to the compensator that is being brought about by this digitization procedure, we have included Figure (24). Note the very large changes that occur in some gains vs. sample rate.

The digitization procedure is essentially routine and no design iteration is required for any of the sample rates evaluated. The design iteration is carried out on the continuous system with the end product being a set of controller weighting matrices, A & B, and estimator noise matrices Q & R. These matrices are easily turned into discrete control laws (or compensators) for any reasonable sample period in a non-iterative manner.

The most difficult part of the design method is obtaining the continuous optimal design. For systems being designed for the first time, the iterations required are on the same order as those required for a classical design. For systems whose continuous design exists and was obtained using classical means, the iterations required to obtain a matching* optimal design is somewhat cumbersome, but the requirement to "match" only exists in a study such as this where it is important to make consistent comparisons.

---

*
actually can't be matched exactly because the order of the continuous compensation is higher for the optimal method.
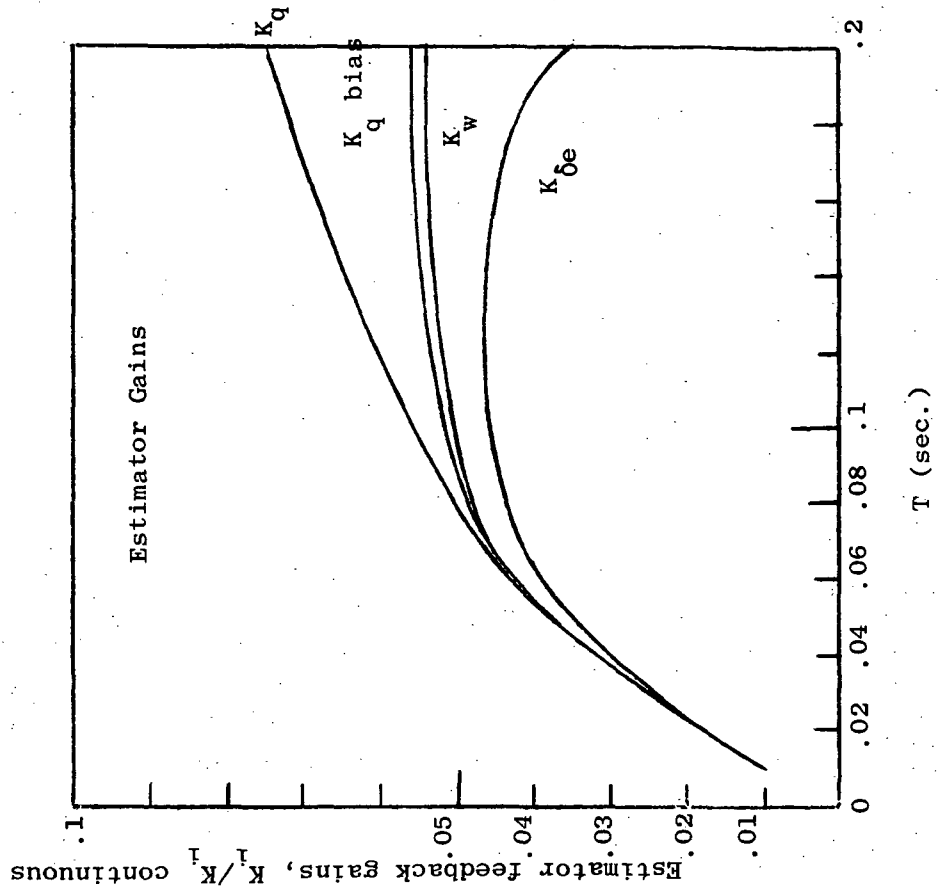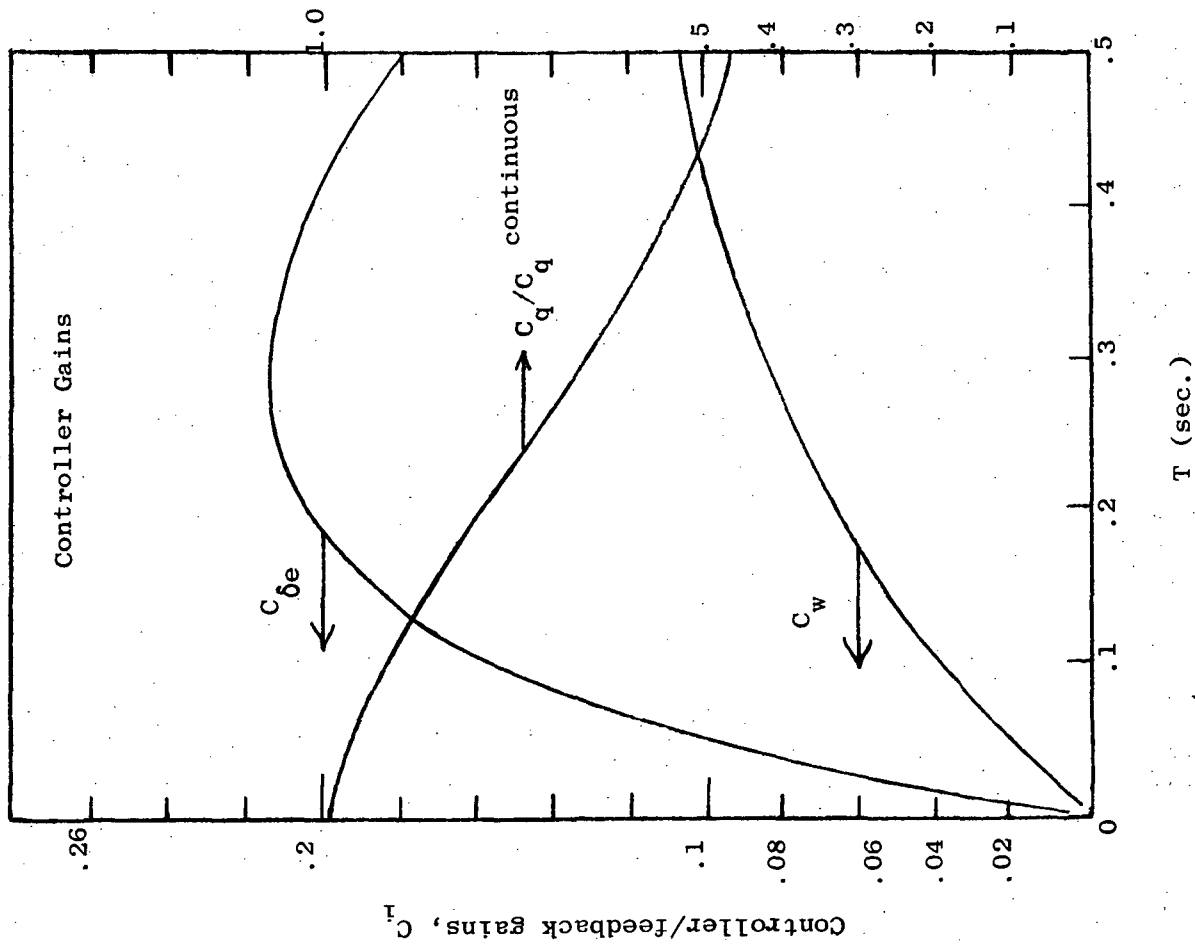
Figure 24 Controller and Estimator Gains Versus Sample Period

2.6 Comparisons of Design Methods

Five different design methods have been evaluated for various modes of the TCV flight control system. For a common comparison of the methods, the fastest loop (inner pitch stabilization) has been evaluated by all of the methods.

Figure 25 shows the equivalent s-plane short period root locations of the discrete systems for four of the design methods and Figures 26 and 27 show the closed loop frequency response characteristics for 5 of the methods. The methods are:

1) Uncompensated s-plane design (section 2.2)

2) Modified s-plane design based on pole fixing with the matched z-transform digitization (section 2.3.1)

3) Modified s-plane design based on frequency response with the matched z-transform digitization(section 2.3.2)

4) Discrete design based on pole fixing (section 2.4)

5) Optimal discrete design (section 2.5)

Figure 25 shows the most severe degradation in stability for the "uncompensated" design method (as expected), a conclusion that is amplified by Figures 26 and 27. For this flight control design problem, the uncompensated design method should not be used with sample rates much slower than 20 cps. Since the system dominant poles are at approximately 1 cps, this represents sampling at 20 times the dominant closed loop roots.

Further comparison of the designs shows a large root movement of the frequency response design but no corresponding change in the frequency response. This arises because the short period root movement is being counteracted by shifts in the other real roots which are not shown and demonstrates the usefulness of the frequency response information in performing a total design evaluation.

With the exception of the uncompensated design, all other design methods would probably be considered acceptable; however, most show some loss of bandwidth at the slow sampling rate (5 cps).
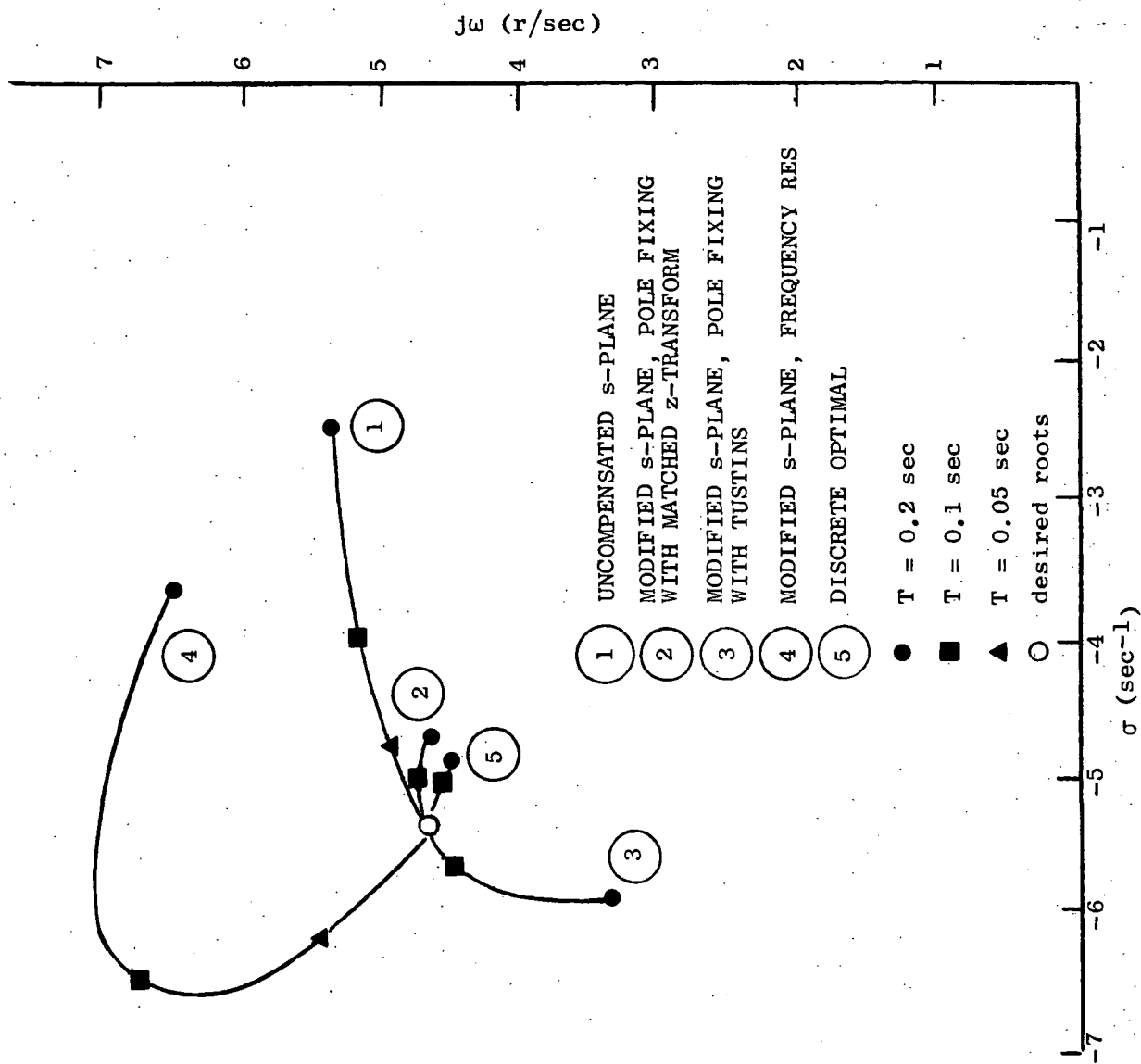
Figure 25 Equivalent S-Plane Short Period Root Locations

-48-
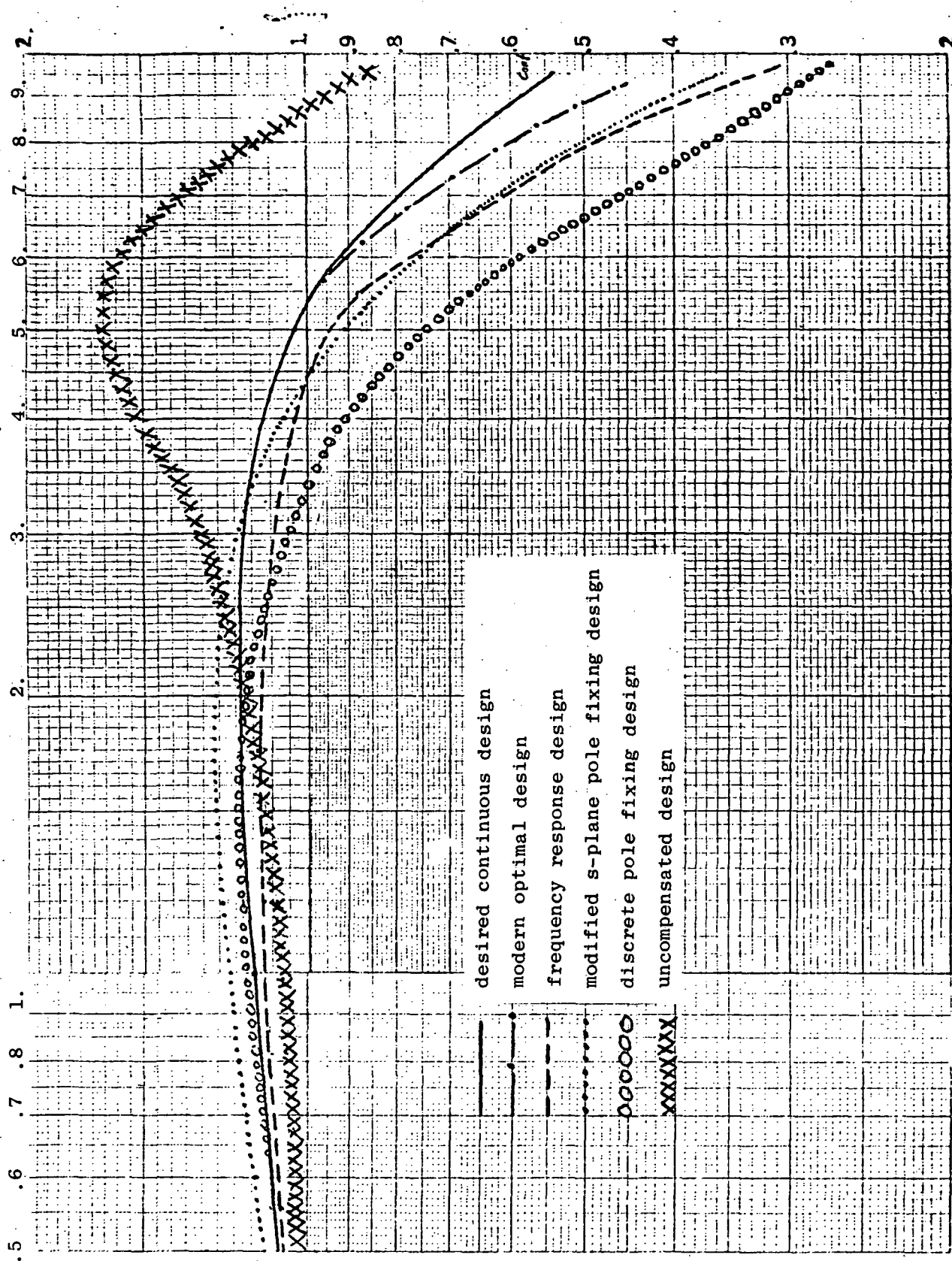
Figure 26 Comparison of Closed Loop Magnitude Frequency
Response by Design for T = .2 Sec.

desired continuous design
modern optimal design
frequency response design
modified s-plane pole fixing design
discrete pole fixing design
uncompensated design

ω (rad./sec.)
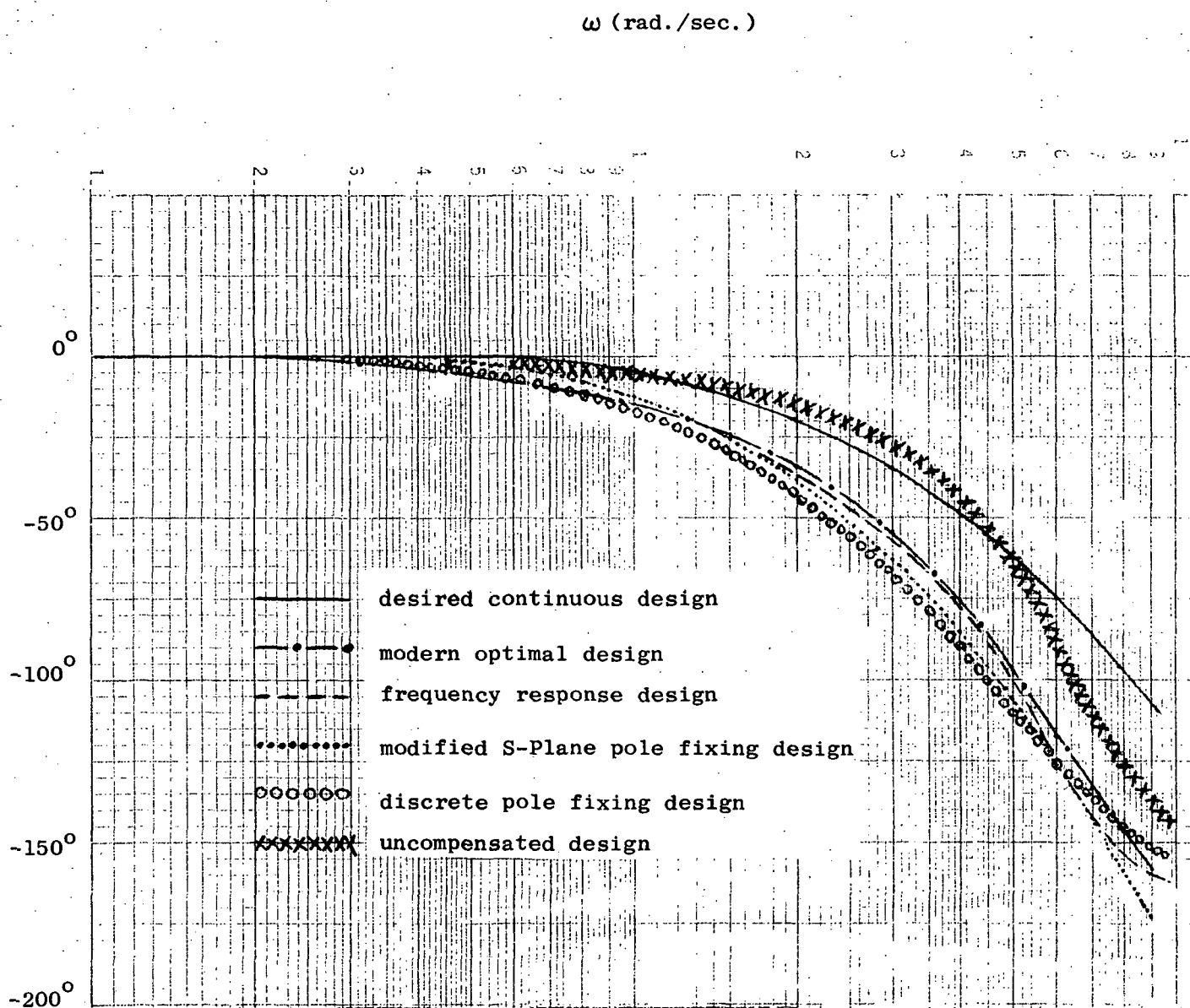
Figure 27   Comparison of Closed Loop Phase Frequency
Response by Design for T = .2 sec.

Since the frequency response design was based on retaining the same gain and phase at crossover (4.1 r/sec) it's interesting to note that the closed loop frequency response information does not match the continuous system at 4.1 r/sec. This is due to the error brought about by the digitization procedure (the matched z-transform), an error that is present for any design method that is based on s-plane results, regardless of whether the hold characteristics are accounted for or not.

Note also however, that accounting correctly for the digitization process is not nearly sufficient in itself to obtain a good design. This is demonstrated by the discrete pole fixing design in Figures 26 and 27, which, except for the uncompensated design, is the worst match to the continuous of all the designs. This design was not shown on the root locus in Figure 25 because it was based on maintaining the z-plane roots at the location which produced no movement of the equivalent s-plane roots. The shift in the frequency response characteristics is due to shifting real root locations which were not taken into account when compensating the system.

Factors other than the accuracy of the method must also be taken into account when evaluating design procedures. Table VIII is included to illustrate these differences. The first column refers to the quality of match to the continuous closed loop bandwidth as evidenced by Figure 26. Intuitive design refers primarily to whether the design iterations are performed in the s-plane or not, which most designers prefer; however, the modern discrete is given a qualified yes because many designers do not consider the weighting matrix selection an intuitive process. The third column refers to whether the digitization effects are evaluated in the z-plane or not. For the s-plane methods, the magnitude of the error is dependent on the frequency placement of the compensation -- the higher the frequencies, the worse the error. This error can always be computed by an analysis such as that performed by this study, but this is not considered to be part of the design method. The fourth column refers to whether any design iterations are required when changing sample rate,

TABLE VIII SUMMARY OF DESIGN METHODS

METHOD	CLOSED LOOP FREQ. RESPONSE ACCURACY (RANK)	INTUITIVE DESIGN	ERROR IN DESIGN METHOD	ITERATIVE DIGITIZATION	ORDER OF COMPENSATION	MINIMUM ω_s/ω DOMINENT VALIDITY
Uncompensated	5	Yes	Yes (very great)	No	1	20
Modified Pole Fix	2	Yes	Yes	Yes	2	10
S-Plane F.R.	3	Yes	Yes	Yes	2	10
Direct Discrete	4	No	None	Yes	2	15
Modern Discrete	1	Yes*	None	No	4	5

*design iteration done in s-plane but weighting matrix selection may not be intuitive.

a feature that is attractive if part of the design exercise is to determine the minimum practical sample rate; hence designs at many sample rates being required. The order of the compensation refers to the complexity of the control mechanization. For all but the modern design, considerable freedom exists in the order of the compensation, although the order tends to increase with slower sampling. For the modern design the compensation order is typically equal to the plant order but can be made equal to the plant minus the number of measurements when using a reduced order estimator. The last column is a somewhat arbitrary attempt to indicate at what sample rates the method can be used. For example the uncompensated design method should not be used at sample rates below 20 times the dominant closed loop poles. These estimates are based primarily on the quality of the closed loop bandwidth match as indicated in Figure 26 and in the more detailed design data in the individual sections. They are valid for the example used in the designs, the 737 TCV pitch stabilization mode, and should be used with some caution for other design problems.

3.0   Roughness

Since the output of a ZOH is constant for an entire sampling period, the control is a series of steps which may be perceived by a pilot through his motion or visual cues as jerkiness or roughness. These effects will be most noticeable in the high frequency modes of the aircraft and become increasingly noticeable as the sample rate decreases.

To evaluate and quantify this effect of digital flight control for varying sample rates, the following designs have been selected for implementation on the Langley motion simulator. The autoland and control wheel steering modes have been selected for this investigation. The autoland mode essentially places the pilot in a monitoring type of function and may produce different reactions compared to the control wheel steering where he will be required to execute various tasks.

The holds to be considered are (Fig. 28) the standard zero order hold (ZOH) for a baseline and the integral hold.
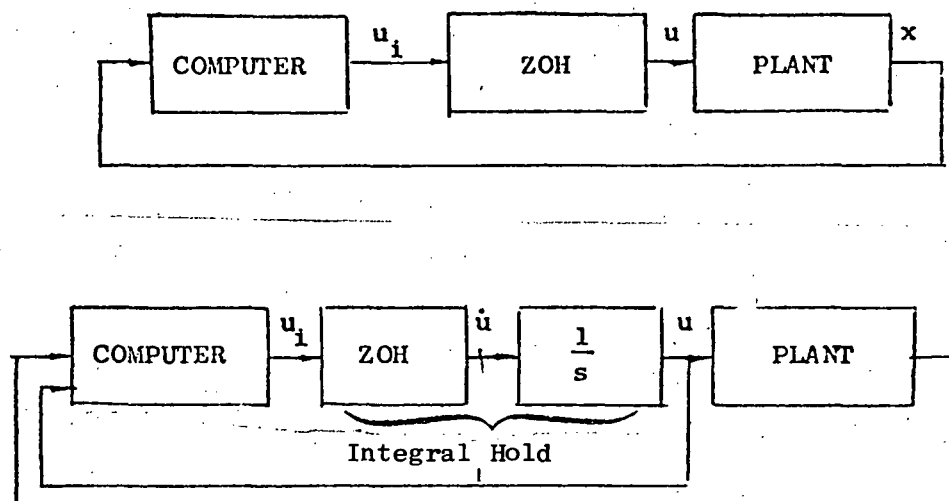
Figure 28   Hold Definition

The integral hold (IGH) is motivated by the desire to eliminate the step changes in u characteristic of the ZOH but to retain its hardware simplicity. Its mechanization simply requires the addition of an anolog integrator between the standard ZOH and the actuators in the aircraft.

Figure 29 combines the different elements of the evaluation and indicates where the different portions of the computations are to be carried out.

The algorithms to be implemented for the hold are:

ZOH: $u(t) = u_i; t_i < t < t_{i+1}$

IGH: $u(t) = \int_0^t u_i dt$

The aircraft model and autopilot for the control wheel steering mode for use with the ZOH is given in Figure 18 with the washout coefficients given in Table II and lead coefficients in Table VII for the sample rates to be used on the CDC 6600.

The aircraft model for the autoland mode is given by Figures 1 and 3 and the additional position state relationship:

$$\dot{h} = w - 207.1 \, \theta$$

The autoland autopilot for use with a ZOH is given in Figure 6. The digital washout coefficients are again given in Table II and the integration by:

$$b_{n+1} = b_n + \frac{T}{2} (a_{n+1} + a_n)$$

For adequate stability with decreasing sample rates, the overall loop gain shown to be 0.85 in Figure 6 was adjusted according to Table IX.

TABLE IX

Autoland Gains

Sampling Rate	Gain
32 cps	0.60
16	0.51
8	0.34
4	0.21
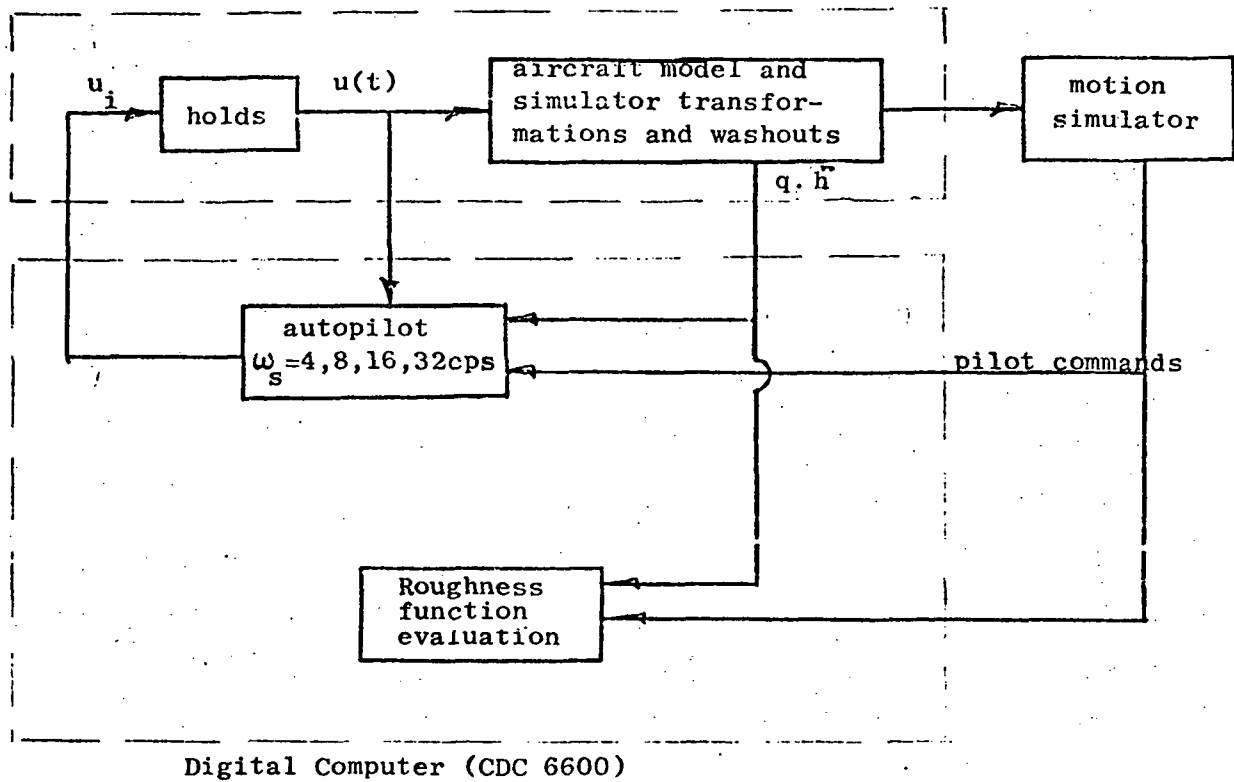
Figure 29   Roughness Simulation Schematic

-56-

For the integral hold, designs are preliminary and need further refinement for good response characteristics. Because of the extra 90° phase lag of the integrator and the additional feed-back from the integrator, the design is more difficult than that for the ZOH. One preliminary design was performed using a modified s-plane approach where an approximation to the delay is contained in the system model. The design was obtained for $\dot\theta$ feedback only so did not represent the full control wheel steering mode. Figure 30 shows the block diagram and defines portions of the compensation.
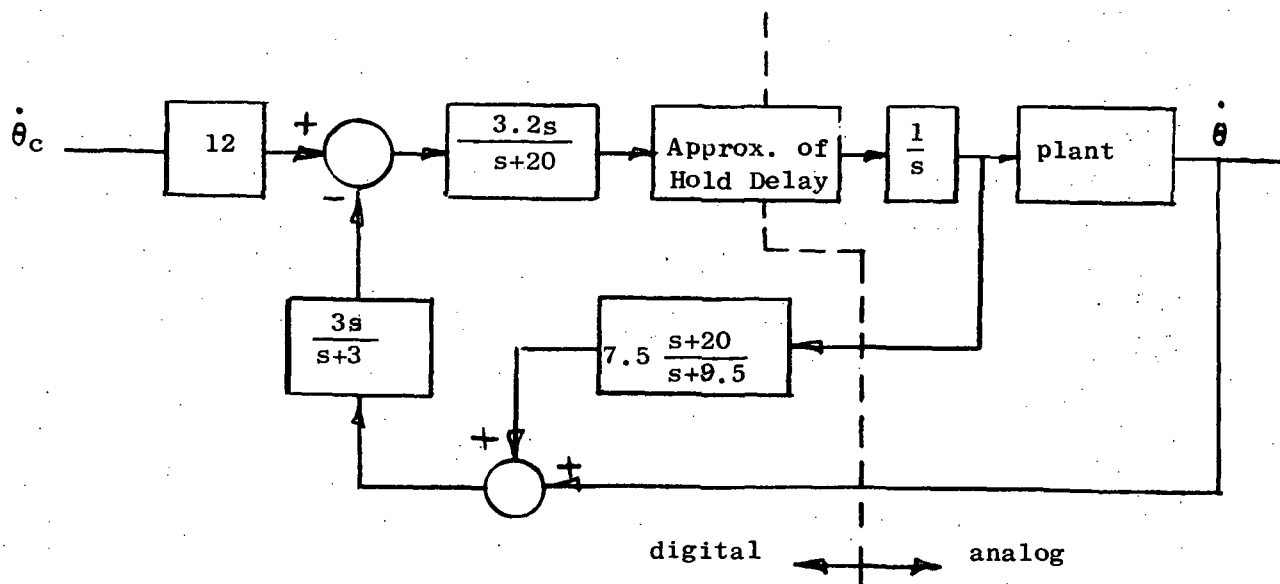
Figure 30   Integral Hold Design

The transient response of this controller obtained from a hybrid simulation with a 10 cps sample rate in the digital portion is shown in Figure 31. It shows that the performance can be made to match that of the system without the extra integrator even though the controller input to the actuator is ramped instead of stepped. Furthermore, the magnitude closed loop frequency response is shown in Figure 32 to match very closely as well. Further design efforts are
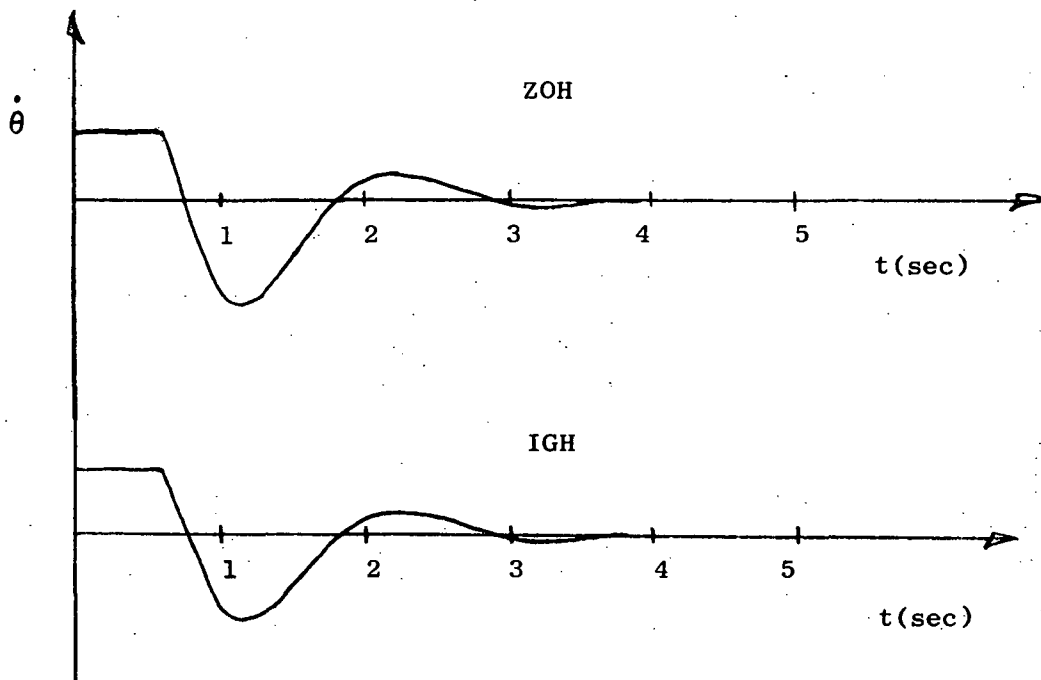
Figure 31   Transient Response of Pitch Stabilization Mode

from Hybrid Simulation

underway to determine compensation for the control wheel steering and autoland modes.
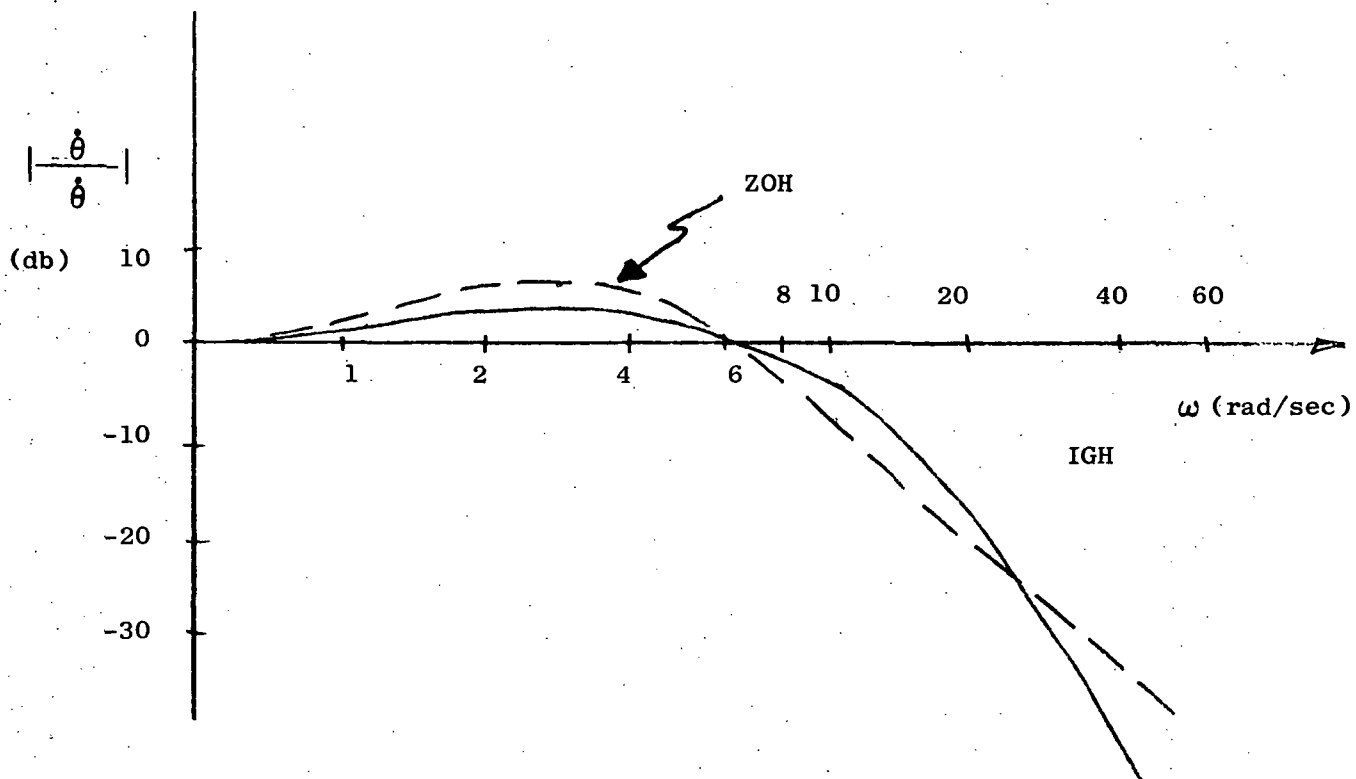
Figure 32 Closed loop Frequency Response Comparison
of the Integral and Conventional Holds

Analytical evaluations of roughness have been proposed [20] and can be used for a quantitative comparison with pilot evaluations; they are:

$$RF_1 = \sum_{i=o}^{N} \left(\frac{\theta_1}{\pi/2}\right)^2 \Delta u^2$$

$$RF_2 = \sum_{i=o}^{N} \left(\frac{\theta_2}{\pi/2}\right)^2 \Delta u^2$$

$$RF_3 = \max\left|\frac{\theta_2}{\pi/2} \Delta u\right|$$

$$RF_4 = \max\left|\frac{\theta_1}{\pi/2} \Delta u\right| .$$

where the terms are defined in Figure 33. These functions are to be evaluated in the digital computer during the simulations.

The exact nature of the evaluations with regards to initial conditions for the autoland, test maneuvers for the control wheel steering, and form of pilot evaluations, have not been determined.
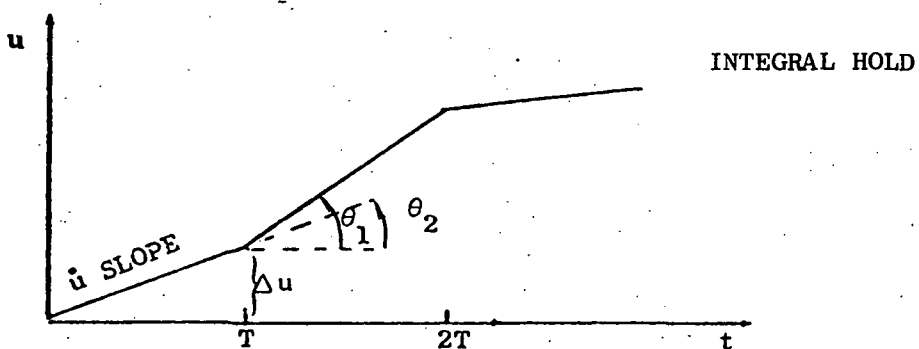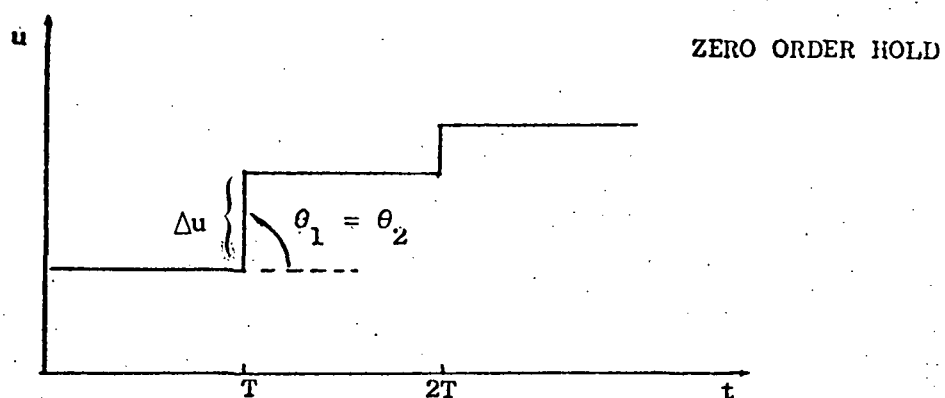
Figure 33   Roughness Function Parameter Definitions

CONCLUSIONS

Discrete Design methods have been compared at various sample rates for several different flight control modes for the Langley TCV Boeing 737. It has been shown that digitization of continuous auto- pilot design leads to a substantial degradation in performance for sample rates slower than 20 Hz (or 20 times the closed loop bandwidth). Modifications to the s-plane design to account for the lag due to sampling improves performance considerably and can be used with confidence at sample rates of 10 Hz (or 10 times the closed loop bandwidth). For sample rates much lower than 10 Hz, a discrete design procedure is advised to eliminate the digitization error present in any s-plane design procedure. A new discrete design procedure has been evaluated which is based on optimal control and estimation techniques. It entails performing the design iterations on the continuous system, then using the resulting weighting matrices in a discrete optimal control procedure. The resulting discrete designs match the continuously designed system better than any other method evaluated and requires no iteration during the discretization procedure, a feature that no other acceptably accurate method possesses.

A test of roughness has been defined and control algorithms determined for the Langley simulator facility with sample rates of 32, 16, 8 & 4 Hz. Preliminary designs are included for the integral hold, a hold which requires the addition of an integrator between the ZOH and the actuator.

Appendix A: Program LEAD

Program LEAD calculates the eigenvalues in the z-plane of a continuous system with a ZOH, actuator dynamics, and a digital controller mechanized in difference equations. An option of the program allows the user to calculate the lead network required at the input of the ZOH to produce given s-plane roots.

Derivation:

A system may be written

$$\dot{x} = A'x + B'u \qquad\qquad A1$$

where

$$x = \begin{bmatrix} x_s \\ x_a \end{bmatrix}$$, a state vector partitioned into the original

states x_s, from $\dot{x} = Ax + Bu$, and x_a, the actuator states

$$A' = \begin{bmatrix} A & B \\ 0 & C \end{bmatrix} ,$$

$$B' = \begin{bmatrix} 0 \\ D \end{bmatrix} \qquad\qquad A2$$

Thus u is the control signal to the actuators whose differential equations are of the form

$$\dot{x} = Ax_s + Bx_a \qquad\qquad A3$$

If the transition matrix is calculated for equation A1

$$x_{n+1} = PX_n + Qu_n \qquad\qquad A4$$

where

$$P = e^{A'T}$$

$$Q = \int_0^T e^{A'\tau} B' d\tau$$

To equation A4 must be added the difference equations of the digital controller. The control is of the form

$$u_n = C_1 x_n + C_2 x_{cn} + C_3 \dot{x}_{sn} \qquad\qquad A5$$

-62-

where x_c is the controller state variables,

$\dot{x}_s$ is the derivative of original state variables such as acceleration. (and $\dot{x}_s = A'x$)

then

$$x_{n+1} = [P + Q(C_1 + C_3 A')] \, x_n + QC_2 x_{cn} \qquad \text{A6}$$

The difference equations can be written

$$x_{cn+1} = M_1 x_{cn} + M_2 x_{cn+1} + M_3 x_n + M_4 x_{n+1} + M_5 \dot{x}_{5n} + M_6 \dot{x}_{sn+1} \qquad \text{A7}$$

The presence of x_{cn+1}, x_{n+1}, x_{sn+1} is due to the existance of these types of terms in most matched 3-transforms.

Now $$\dot{x}_{sn+1} = A' x_{n+1} \qquad \text{A8}$$

which can be rewritten using A6

$$\dot{x}_{sn+1} = A'[P + Q(C_1 + C_3 A')] \, x_n + A' QC_2 x_{cn} \qquad \text{A9}$$

and finally

$$x_{cn+1} = (I-M_2)^{-1} \left\{ M_3 + (M_4 + M_6 A')[P + Q(C_1 + C_3 A')] + M_5 A' \right\} x_n$$

$$+ (I-M_2)^{-1} \left\{ M_1 + (M_4 + M_6 A')QC_2 \right\} x_{cn} \qquad \text{A10}$$

Thus, given the state definition A2, A3, the sampling interval T, the control law A5, and the difference equations A7, LEAD solves for the eigenvalues of the matrix

$$\begin{bmatrix} P + Q(C_1 + C_3 A') & QC_2 \\ (I-M_2)^{-1} \left\{ M_3 + (M_4 + M_6 A')[P + Q(C_1 + QC_3) + M_5 A'] \right\} & (I-M_2)^{-1}[M_1 + (M_4 + M_6 A')QC_2] \end{bmatrix}$$

To calculate the lead network required to fix a specific root in the s-plane, the program first computes the poles and zeroes of the system in the z-plane. It then transforms the desired root into the

z-plane, calculate the lead angle deficiency, and places the pole of the lead network from this. The gain is computed by standard root-locus methods.

The user must program 3 FORTRAN subroutines: size, diffeq, and plant. They define respectively the size of various arrays, the difference equation matrices, and the state equations of the plant and actuators. A listing follows of the main program and relevant subroutines.

```
      IMPLICIT REAL (K,L,M)
      REAL*8 F,ICNT,INT,GN,C9,ACL
      REAL*8 SRE,SIM,CWI,CWR
      REAL*8 DLCG,DSORT,DATAN
      DIMENSION ICNT(20),INT(20),GN(10,10),D9(20),CWR(10),CWI(10)
     5   ,TINV(10,10),ACL(10,10)
      DIMENSION RVEC(10,10),VECRN(10,10),VECIN(10,10),VECR(10,10)
     1   ,VECI(10,10),VRV(10),VIV(10),VRRV(10),VRIV(10)
      DIMENSION APRIME(10,10),BPRIME(10,10),P(10,10),Q(10,10)
     1   ,C1(10,10),C2(10,10),C3(10,10),M1(10,10),M2(10,10)
     2   ,M3(10,10),M4(10,10),M5(10,10),M6(10,10)
     3   ,A(10,10),B(10,10),C(10,10),D(10,10),DNUM(10,10),TEM5BA(10,10)
     4   ,TEMAA(10,10),TEM2AA(10,10),TEMBA(10,10),TEMAB(10,10)
     2   ,V1(20),V2(20),TEM3EA(10,10),TEM3B(10,10),TEM2BB(10,10)
     6   ,TEM2AB(10,10),F(10,10),TEM2BA(10,10),TEM4BA(10,10)
      DATA APRIME/100*0./,BPRIME/100*0./,P/100*0./,Q/100*0./
     3   ,C1/100*0./,C2/100*C./,C3/100*0./,M1/100*0./,M2/100*0./
     2   ,M3/100*0./,M4/100*0./,M5/100*0./,M6/100*0./
      DATA A/100*0./,B/100*0./,C/100*0./
      CALL SIZE(NPLANT,NDIG,NC,NACT)
      NS=NPLANT+NACT
      NSTCT=NS+NDIG
      NSTOT2=2*NSTOT
      CALL DOIT(NPLANT,NDIG,NC,NACT,NS,NSTOT,NSTOT2,
     1 ICNT,INT,GN,D9,CWR,CWI,TINV,ACL,RVEC,VECRN,VECIN,VECR,
     2 VECI,VRV,VIV,VRRV,VRIV,APRIME,BPRIME,P,Q,C1,C2,C3,M1,M2,M3,M4,
     3 M5,M6,A,B,C,D,TEM5BA,TEMAA,TEM2AA,TEMBA,TEMAB,V1,V2,
     4 TEM3BA,TEMBB,TEM2BB,TEM2AB,F,TEM2BA,TEM4BA,DNUM)
      RETURN
      END
      SUBROUTINE DOIT(NPLANT,NDIG,NC,NACT,NS,NSTOT,NSTOT2,
     1 ICNT,INT,GN,D9,CWR,CWI,TINV,ACL,RVEC,VECRN,VECIN,VECR,
     2 VECI,VRV,VIV,VRRV,VRIV,APRIME,BPRIME,P,Q,C1,C2,C3,M1,M2,M3,M4,
     3 M5,M6,A,B,C,D,TEM5BA,TEMAA,TEM2AA,TEMBA,TEMAB,V1,V2,
     4 TEM3BA,TEMBB,TEM2BB,TEM2AB,F,TEM2BA,TEM4BA,DNUM)
      IMPLICIT REAL (K,L,M)
      REAL*8 F,ICNT,INT,GN,C9,ACL
      REAL*8 SRE,SIM,CWI,CWR
      REAL*8 DLCG,DSQRT,DATAN
      COMMON/T/TSAMP,CPCLES,CZERCS
      DIMENSION ZERO(2,8),PCLE(2,8)
      DIMENSION ICNT(NSTOT2),INT(NSTOT2),GN(NSTOT,NSTOT),D9(NSTOT2),
     1 CWR(NSTOT),CWI(NSTOT),TINV(NDIG,NDIG),ACL(NSTOT,NSTOT),
     2 RVEC(NSTOT,NSTOT),VECRN(NSTOT,NSTOT),VECIN(NSTOT,NSTOT),
     3 VECR(NSTOT,NSTOT),VECI(NSTOT,NSTOT),VRV(NSTOT),VIV(NSTOT),
     4 VRRV(NSTOT),VRIV(NSTOT),APRIME(NS,NS),BPRIME(NS,NC),
     5 P(NS,NS),Q(NS,NC),C1(NC,NS),C2(NC,NDIG),C3(NC,NS)
      DIMENSION M1(NDIG,NDIG),M2(NDIG,NDIG),M3(NDIG,NS),M4(NDIG,NS),
     1 M5(NDIG,NS),M6(NDIG,NS),A(NPLANT,NPLANT),B(NPLANT,NC),
     2 C(NACT,NACT),D(NACT,NC),TEM5BA(NDIG,NS),TEMAA(NS,NS),
     3 TEM2AA(NS,NS),TEMBA(NDIG,NS),TEMAB(NS,NDIG),V1(NSTOT2),
     4 V2(NSTOT2),TEM3BA(NDIG,NS),TEM3B(NDIG,NDIG),TEM2BB(NDIG,NDIG),
     5 TEM2AB(NS,NDIG),F(NSTOT,NSTOT),TEM2BA(NDIG,NS),TEM4BA(NDIG,NS)
     6 ,DNUM(NACT,NC)
      CALL PLANT(NPLANT,NDIG,NC,NACT,NS,NSTOT,NSTOT2,
     1 ICNT,INT,GN,D9,CWR,CWI,TINV,ACL,RVEC,VECRN,VECIN,VECR,
     2 VECI,VRV,VIV,VRRV,VRIV,APRIME,BPRIME,P,Q,C1,C2,C3,M1,M2,M3,M4,
     3 M5,M6,A,B,C,D,TEM5BA,TEMAA,TEM2AA,TEMBA,TEMAB,V1,V2,
     4 TEM3BA,TEMBB,TEM2BB,TEM2AB,F,TEM2BA,TEM4BA,DNUM)
1009  CALL PROMPT('ZERO? ',C,10)
```

-65-

```
CCCCC  REAC CCMFENSATION ZERC (PCSITIVE SIGN)
       READ(10,*) CZEROS
  1    CCNTINUE
       CALL FRCMPT('INS? ',5,10)
CCCCC
CCCCC  READ INSTRUCTIONS
CCCCC  INS = 1,2,3, OR 4 (INTEGER)
CCCCC  TSAMP = SAMPLING INTERVAL (SECUNDS)
CCCCC  TFE THIRC AND FOURTH VARIABLES READ HAVE MEANINGS DEPENDENT
CCCCC      CN THE VALUE OF INS
CCCCC  INS=1: RCCTS IN THE Z PLANE AND S PLANE WILL BE FOUND FOR
CCCCC      TFE SYSTEM WITH AN INPUTTED GAIN AND COMPENSATION
CCCCC      PCLE AND ZERO.  THE THIRD VARIABLE IS THE GAIN.  IT
CCCCC      MULTIPLIES ALL THE ELEMENTS OF THE DNOM MATRIX.  THE
CCCCC      FCURTH VARIABLE IS THE COMPENSATION POLE (POSITIVE
CCCCC      SIGN).  IF NC CCMPENSATION IS DESIRED, SET THE POLE
CCCCC      LOCATION AT THE ZEFC LCCATION.  THE ROOTS WILL THEN
CCCCC      INCLUDE AN UNCCUPLEC ONE CORRESPONDING TO THE
CCCCC      CCMPENSATICN.
CCCCC  INS=2: TFE GAIN AND PCLE LCCATION WILL BE CALCULATED THAT
CCCCC      WILL GUARANTEE FARTICULAR RODTS IN THE S PLANE.  THE
CCCCC      DESIRED S PLANE ROOT IS INPUTTED AS THE THIRD AND FOURTH
CCCCC      VARIABLES (REAL AND IMAGINARY).  AS A CHECK, THE
CCCCC      ROOTS ARE CALCULATED WITH THIS COMPUTED COMPENSATION AND
CCCCC      GAIN.  THIS CAN BE LSED TO CHECK ON THE LOCATION OF
CCCCC      CTFER ROOTS WHCSE LCCATIONS WERE NOT SPECIFIED.
CCCCC      TFIS OPTICN WILL WCRK CURRENTLY ONLY FOR 1 ACTUATOR
CCCCC      THAT INFLUENCES THE STATES THROUGH ONE NON-ZERO ELEMENT
CCCCC      CF DNOM.  ANY CTFER FORMULATION WILL GIVE UNPREDICTABLE
CCCCC      RESULTS IN THIS VERSION.
CCCCC  INS=3: THIS PERFORMS TFE SAME COMPUTATION AS FOR INS=2.
CCCCC      THIS CAN BE USED CNLY AFTER INS=2 HAS BEEN SPECIFIED
CCCCC      FCR A PARTICULAR ZERO LOCATION AND SAMPLING INTERVAL.
CCCCC      THIS OPTICN EXISTS TC ELIMINATE SOME COMPUTATION THAT
CCCCC      WAS PERFORMED FREVICUSLY.
CCCCC  INS=4: RETURNS TO A PRCMPT FOR A NEW ZERO.  THE SECOND, THIRD
CCCCC      AND FOURTH VARIABLES MUST BE INPUTTED, BUT ARE IGNORED.
CCCCC
       READ(10,*) INS,TSAMP,SRFNT,SIPNT
       GO TO (99,44,166,1009),INS
  99   CGAIN=SRFNT
       CPCLES=SIFNT
       GO TO 199
  44   GAIN=1.
       CPCLES=CZEROS
       CALL CMAT(D,DNOM,NACT,NC,GAIN)
       CALL CNTRL(NPLANT,NCIC,NC,NACT,NS,NSTOT,NSTOT2,
      1 ICNT,INT,GN,D9,CWR,CWI,TINV,ACL,RVEC,VECRN,VECIN,VECR,
      2 VECI,VRV,VIV,VRRV,VRIV,AFRIME,BPRIME,F,G,C1,C2,C3,H1,M2,M3,M4,
      3 M5,M6,A,B,C,D,TEM5BA,TEMAA,TEM2AA,TEMBA,TEMAB,V1,V2,
      4 TEM3BA,TEMBB,TEM2BB,TEM2AB,F,TEM2BA,TEM4BA,DNOM)
       CO 1403 J=1,NSTOT
       R=CWR(J)**2+CWI(J)**2
       IF (R .GT. 1. ) GC TC 1403
       XR=CWR(J)
       YI=CWI(J)
       CO TO 1409
 1403  CCNTINUE
 1409  GAIN=0.
       CALL CMAT(D,DNOM,NACT,NC,GAIN)
       CALL CNTRL(NPLANT,NCIC,NC,NACT,NS,NSTOT,NSTOT2,
```

```
    1 ICNT,INT,GN,D9,ChR,ChI,TINV,ACL,RVEC,VECRN,VECIN,VECR,
    2 VECI,VRV,VIV,VFRV,VRIV,APRIME,BPRIME,P,Q,C1,C2,C3,M1,M2,M3,M4,
    3 M5,M6,A,B,C,D,TEM5BA,TEMAA,TEM2AA,TEMBA,TEMAB,V1,V2,
    4 TEM3BA,TEMBB,TEM2BB,TEM2AB,F,TEM2BA,TEM4BA,DNUM)
      SF=1.
      DO 404 I=1,NSTOT
      SF=SF/DSQRT((XR-ChR(I))**2+(YI-CWI(I))**2)
      PCLE(1,I)=CWR(I)
  404 POLE(2,I)=CWI(I)
      GAIN=1.E10
      CALL CMAT(D,DNOM,NACT,NC,GAIN)
      CALL CNTRL(NPLANT,NDIG,NC,NACT,NS,NSTOT,NSTOT2,
    1 ICNT,INT,GN,D9,ChR,ChI,TINV,ACL,RVEC,VECRN,VECIN,VECR,
    2 VECI,VRV,VIV,VRRV,VRIV,APRIME,BPRIME,P,Q,C1,C2,C3,M1,M2,M3,M4,
    3 M5,M6,A,B,C,D,TEM5BA,TEMAA,TEM2AA,TEMBA,TEMAB,V1,V2,
    4 TEM3BA,TEMBB,TEM2BB,TEM2AB,F,TEM2BA,TEM4BA,DNUM)
      NZ=0
      DO 505 I=1,NSTOT
      IF (CWR(I)**2+CWI(I)**2 .GT. 2) GO TO 505
      NZ=NZ+1
      ZERO(1,NZ)=CWR(I)
      ZERO(2,NZ)=CWI(I)
  505 CONTINUE
      DO 609 I=1,NZ
  609 SF=SF*SQRT((XR-ZERO(1,I))**2+(YI-ZERO(2,I))**2)
  166 CZEROZ=EXP(-TSAMP*CZEROS)
      ZRPNT=EXP(SRPNT*TSAMP)*COS(SIPNT*TSAMP)
      ZIPNT=EXP(SRPNT*TSAMP)*SIN(SIPNT*TSAMP)
      CALL LEAD(ZRPNT,ZIPNT,NSTOT,POLE,NZ,ZERO,CGAIN,CPOLEZ,PHI
    1 ,CZEROZ,SF)
      CPOLES=-ALOG(CPOLEZ)/TSAMP
      WRITE(6,5440) CPOLES,CGAIN
 5440 FORMAT(' POLE ',G15.6,' GAIN ',G15.6)
  199 CONTINUE
      CALL CMAT(D,DNOM,NACT,NC,CGAIN)
      CALL CNTRL(NPLANT,NDIG,NC,NACT,NS,NSTOT,NSTOT2,
    1 ICNT,INT,GN,D9,ChR,ChI,TINV,ACL,RVEC,VECRN,VECIN,VECR,
    2 VECI,VRV,VIV,VRRV,VRIV,APRIME,BPRIME,P,Q,C1,C2,C3,M1,M2,M3,M4,
    3 M5,M6,A,B,C,D,TEM5BA,TEMAA,TEM2AA,TEMBA,TEMAB,V1,V2,
    4 TEM3BA,TEMBB,TEM2BB,TEM2AB,F,TEM2BA,TEM4BA,DNUM)
    8 FORMAT(' ',G15.6,15X,G15.6)
   10 FORMAT(' ',4G15.6)
      DO 960 J=1,NSTOT
      SRE=DLOG(DSQRT(CWR(J)**2+CWI(J)**2))/TSAMP
      SIM=DATAN(CWI(J)/CWR(J))/TSAMP
      IF (CWI(J) .EQ. 0.D0) GO TO 4974
      WRITE(6,10) CWR(J),CWI(J),SRE,SIM
      GO TO 960
 4974 WRITE(6,8) CWR(J),SRE
  960 CONTINUE
      GO TO 1
   46 RETURN
      END
C
C
C
C
C
C
C
C
```

-67-

```
C
C
      . SLBROUTINE CNTRL(NPLANT,NDIG,NC,NACT,NS,NSTOT,NSTOT2,
     1 ICNT,INT,GN,D9,CWR,CWI,TINV,ACL,RVEC,VECRN,VECIN,VECR,
     2 VECI,VRV,VIV,VRRV,VRIV,APRIME,BPRIME,P,Q,C1,C2,C3,M1,M2,M3,M4,
     3 M5,M6,A,B,C,D,TEM5BA,TEMAA,TEM2AA,TEMBA,TEMAB,V1,V2,
     4 TEM3BA,TEMBB,TEM2BB,TEM2AB,F,TEM2BA,TEM4BA,DNOM)
       IMPLICIT REAL (K,L,M)
       REAL*8 F,ICNT,INT,GN,CS,ACL
       REAL*8 SRE,SIM,CWI,CWR
       REAL*8 DLCG,DSQRT,DATAN
       CCMMON/T/TSAMP,CFCLES,CZERCS
       DIMENSICN ICNT(NSTOT2),INT(NSTOT2),GN(NSTOT,NSTOT),D9(NSTOT2),
     1 CWR(NSTOT),CWI(NSTOT),TINV(NDIG,NDIG),ACL(NSTOT,NSTOT),
     2 RVEC(NSTCT,NSTOT),VECRN(NSTOT,NSTOT),VECIN(NSTOT,NSTOT),
     3 VECR(NSTCT,NSTOT),VECI(NSTOT,NSTOT),VRV(NSTOT),VIV(NSTOT),
     4 VRRV(NSTCT),VRIV(NSTCT),APRIME(NS,NS),BPRIME(NS,NC),
     5 P(NS,NS),G(NS,NC),C1(NC,NS),C2(NC,NDIG),C3(NC,NS)
       DIMENSICN M1(NDIG,NDIG),M2(NDIG,NDIG),M3(NDIG,NS),M4(NDIG,NS),
     1 M5(NDIG,NS),M6(NDIG,NS),A(NPLANT,NPLANT),B(NPLANT,NC),
     2 C(NACT,NACT),D(NACT,NC),TEM5BA(NDIG,NS),TEMAA(NS,NS),
     3 TEM2AA(NS,NS),TEMBA(NDIG,NS),TEMAB(NS,NDIG),V1(NSTOT2),
     4 V2(NSTOT2),TEM3BA(NDIG,NS),TEMBB(NDIG,NDIG),TEM2BB(NDIG,NDIG),
     5 TEM2AB(NS,NDIG),F(NSTOT,NSTOT),TEM2BA(NDIG,NS),TEM4BA(NDIG,NS)
     6 ,DNOM(NACT,NC)
C
       CALL CIFFEQ(NPLANT,NDIG,NC,NACT,NS,NSTOT,NSTOT2,
     1 ICNT,INT,GN,D9,CWR,CWI,TINV,ACL,RVEC,VECRN,VECIN,VECR,
     2 VECI,VRV,VIV,VRRV,VRIV,APRIME,BPRIME,P,Q,C1,C2,C3,M1,M2,M3,M4,
     3 M5,M6,A,B,C,D,TEM5BA,TEMAA,TEM2AA,TEMBA,TEMAB,V1,V2,
     4 TEM3BA,TEMBB,TEM2BB,TEM2AB,F,TEM2BA,TEM4BA,DNOM)
C
       DO 91 I= 1,NPLANT
       DC 90 J= 1,NPLANT
   90 APRIME(I,J)= A(I,J)
       DC 91 J= 1,NC
   91 APRIME(I,J+NPLANT)= B(I,J)
       DO 94 I= 1,NACT
       CC 94 J=1,NACT
   94 APRIME(I+NPLANT,J+NPLANT)= C(I,J)
C
       DC 96 I=1,NACT
       DO 96 J=1,NC
   96 BPRIME(I+NPLANT,J)=D(I,J)
       CALL FGPC(APRIME,BPRIME,P,C,NS,NC,TSAMP)
       CALL MMULT(C3,APRIME,TEM5BA,NC,NS,NS)
       CALL MACC(TEM5BA,C1,TEMBA,NC,NS,0)
       CALL MMULT(C,TEM5BA,TEMAA,NS,NC,NS)
       CALL MACC(TEMAA,P,TEMAA,NS,NS,0)
       CALL MMULT(Q,C2,TEMAB,NS,NC,NDIG)
       CALL MATIN(TINV,NDIG,1)
       CALL MACC(TINV,M2,TINV,NDIG,NDIG,1)
       CALL MINV(NDIG*NDIG,TINV,NDIG,D1,V1,V2)
       CALL MMULT(M6,APRIME,TEM2BA,NDIG,NS,NS)
       CALL MACC(TEM2BA,M4,TEM2BA,NDIG,NS,0)
       CALL MMULT(TEM2BA,TEMAA,TEM3BA,NDIG,NS,NS)
       CALL MMULT(M5,APRIME,TEM4BA,NDIG,NS,NS)
       CALL MACC(TEM4BA,TEM3BA,TEM3BA,NDIG,NS,0)
       CALL MACC(TEM3BA,M3,TEM3BA,NDIG,NS,0)
       CALL MMULT(TINV,TEM3BA,TEMBA,NDIG,NDIG,NS)
       CALL MMULT(Q,C2,TEM2AB,NS,NC,NDIG)
```

-68-

```
      CALL MMULT(TEM2BA,TEM2AB,TEM2BB,NDIG,NS,NDIG)
      CALL MADD(TEM2BB,M1,TEM2BB,NDIG,NDIG,0)
      CALL MMULT(TINV,TEM2BB,TEMBB,NDIG,NDIG,NDIG)
      DO 125 I=1,NS
      DO 125 J=1,NS
 125  F(I,J)=TEMAA(I,J)
      DO 76 I=1,NDIG
      DO 76 J=1,NS
      F(J,I+NS)=TEMAB(J,I)
  76  F(I+NS,J)=TEMBA(I,J)
      DO 77 I=1,NDIG
      DO 77 J=1,NDIG
  77  F(I+NS,J+NS)=TEMBB(I,J)
C*******************************************
      CALL BALANC (NSTOT,NSTOT,F,ILOW,IHIGH,D9)
      CALL ELMHES (NSTOT,NSTOT,ILOW,IHIGH,F,INT)
      CALL HQR2 (NSTOT,NSTOT,ILOW,IHIGH,F,CWR,CWI,ACL,ICNT,&46)
C*********************************************
  46  RETURN
      END
C
C
C
C
C
C
C
C
C
C
C
      SUBROUTINE LEAD(XR,YI,NPOLES,POLE,NZEROS,ZERO,GAIN,COMPP,PHI,
     1 COMPZ,SF)
      DIMENSION POLE(2,8),ZERO(2,8)
      ANGLE=0.
      GAIN=1.
      IF(NPOLES.EQ.0) GO TO 15
      DO 10 I=1,NPOLES
      GAIN=GAIN*SQRT((XR-POLE(1,I))**2+(YI-POLE(2,I))**2)
      TEMP=ATAN((YI-POLE(2,I))/(XR-POLE(1,I)))
      IF(POLE(1,I).GT.XR) TEMP=3.141592+TEMP
  10  ANGLE=ANGLE+TEMP
  16  FORMAT(7F10.2)
  15  IF(NZEROS.EQ.0) GO TO 25
      DO 20 I=1,NZEROS
      GAIN=GAIN/(SQRT((XR-ZERO(1,I))**2+(YI-ZERO(2,I))**2))
      TEMP=ATAN((YI-ZERO(2,I))/(XR-ZERO(1,I)))
      IF(ZERO(1,I).GT.XR) TEMP=3.141592+TEMP
  20  ANGLE=ANGLE-TEMP
  25  PHI = ANGLE+3.141592
      PHIZ=ATAN(YI/(XR-COMPZ))
      IF(COMPZ.GT.XR) PHIZ=3.141592+PHIZ
      COMPP = XR - YI/TAN(PHIZ-PHI)
      GAIN=GAIN* SQRT((XR-COMPP)**2+(YI)**2)
      GAIN=SF*GAIN/( SQRT((XR-COMPZ)**2+(YI)**2) )
      GAIN=GAIN*(1.-COMPZ)/(1.-COMPP)
      RETURN
      END
C
C
C
C
```

```
C
C
C
C
C
C

      SUBROUTINE DMAT(D,DNOM,NACT,NC,GAIN)
      DIMENSION DNOM(NACT,NC),D(NACT,NC)
      DO 10 I=1,NACT
      DO 10 J=1,NC
10    D(I,J)=DNOM(I,J)*GAIN
      RETURN
      END
```

```
      SUBROUTINE SIZE(NPLANT,NDIG,NC,NACT)
CCCCC
CCCCC SIZE IS A USER-WRITTEN PROGRAM THAT DETERMINES THE SIZE OF
CCCCC THE SYSTEM.  IT SHOULD BE PROGRAMMED AS IN THIS EXAMPLE.
CCCCC NPLANT = THE NUMBER OF DIFFERENTIAL EQUATIONS OF THE PLANT
CCCCC NDIG = THE NUMBER OF DIFFERENCE EQUATION IN THE CONTROL
CCCCC NC = THE NUMBER OF CONTROLS
CCCCC NACT = THE NUMBER OF ACTUATOR DIFFERENTIAL EQUATIONS.
CCCCC      NOTE:   THIS MEANS THAT NPLANT DOES NOT INCLUDE ANY
CCCCC      ACTUATOR DYNAMICS
CCCCC THE PROGRAM SHOWN HERE IS FOR THE LONGITUDINAL ATTITUDE
CCCCC CONTROL-WHELL STEERING PROBLEM DISCUSSED IN THE BODY OF THE
CCCCC REPORT
CCCCC
      NPLANT=3
      NDIG=3
      NACT=1
      NC=1
      RETURN
      END
C
C
C
C
C
C
C
C
C
C
C
C
      SUBROUTINE PLANT(NPLANT,NDIG,NC,NACT,NS,NSTOT,NSTOT2,
     1 ICNT,INT,GN,D9,CWR,CWI,TINV,ACL,RVEC,VECRN,VECIN,VECR,
     2 VECI,VRV,VIV,VREV,VRIV,APRIME,BPRIME,P,Q,C1,C2,C3,M1,M2,M3,M4,
     3 M5,M6,A,B,C,D,TEM5BA,TEMAA,TEM2AA,TEMBA,TEMAB,V1,V2,
     4 TEM3BA,TEMBB,TEM2BB,TEM2AB,F,TEM2BA,TEM4BA,DNOM)
      IMPLICIT REAL (K,L,M)
      REAL*8 F,ICNT,INT,GN,D9,ACL
      REAL*8 SRE,SIM,CWI,CWR
      REAL*8 DLOG,DSQRT,DATAN
      COMMON/T/TSAMP,CPOLES,CZEROS
      DIMENSION ZERO(2,8),POLE(2,8)
      DIMENSION ICNT(NSTOT2),INT(NSTOT2),GN(NSTOT,NSTOT),D9(NSTOT2),
     1 CWR(NSTOT),CWI(NSTOT),TINV(NDIG,NDIG),ACL(NSTOT,NSTOT),
     2 RVEC(NSTOT,NSTOT),VECRN(NSTOT,NSTOT),VECIN(NSTOT,NSTOT),
     3 VECR(NSTOT,NSTOT),VECI(NSTOT,NSTOT),VRV(NSTOT),VIV(NSTOT),
     4 VREV(NSTOT),VRIV(NSTOT),APRIME(NS,NS),BPRIME(NS,NC),
     5 P(NS,NS),Q(NS,NC),C1(NC,NS),C2(NC,NDIG),C3(NC,NS)
      DIMENSION M1(NDIG,NDIG),M2(NDIG,NDIG),M3(NDIG,NS),M4(NDIG,NS),
     1 M5(NDIG,NS),M6(NDIG,NS),A(NPLANT,NPLANT),B(NPLANT,NC),
     2 C(NACT,NACT),D(NACT,NC),TEM5BA(NDIG,NS),TEMAA(NS,NS),
     3 TEM2AA(NS,NS),TEMBA(NDIG,NS),TEMAB(NS,NDIG),V1(NSTOT2),
     4 V2(NSTOT2),TEM3BA(NDIG,NS),TEMBB(NDIG,NDIG),TEM2BB(NDIG,NDIG),
     5 TEM2AB(NS,NDIG),F(NSTOT,NSTOT),TEM2BA(NDIG,NS),TEM4BA(NDIG,NS)
     6 ,DNOM(NACT,NC)
CCCCC
CCCCC PLANT IS A USER-WRITTEN PROGRAM THAT DETERMINES THE
CCCCC DIFFERENTIAL EQUATION OF THE PLANT.  MORE SPECIFICALLY IT
CCCCC DEFINES THE MATRICES A,B,C, AND DNOM.  THE ROUTINE IS CALLED
CCCCC ONCE PER RUN, AND THEREFORE MAY CONTAIN READ STATEMENTS AND
CCCCC THE LIKE.
```

```
CCCCC THE PROGRAM SHOWN HERE IS FOR THE LONGITUDINAL ATTITUDE
CCCCC CONTROL-WHELL STEERING PROBLEM DISCUSSED IN THE BODY OF THE
CCCCC REPORT
CCCCC
       A(1,1)=-6.28287E-1
       A(2,1)=-3.27919E-3
       A(1,2)=207.064
       A(2,2)=-4.49954E-1
       A(3,2)=1.
       B(1,1)=-1.40888E-1
       B(2,1)=-1.73928E-2
       C(1,1)=-10.
       DNOM(1,1)=10.
       RETURN
       END
C
C
C
C
C
C
C
C
C
C
       SUBROUTINE DIFFEQ(NPLANT,NDIG,NC,NACT,NS,NSTOT,NSTOT2,
      1 ICNT,INT,GN,D9,CWR,CWI,TINV,ACL,RVEC,VECRN,VECIN,VECR,
      2 VECI,VRV,VIV,VPRV,VPIV,APPIME,BPPIME,P,Q,C1,C2,C3,M1,M2,M3,M4,
      3 M5,M6,A,B,C,D,TEM5BA,TEMAA,TEM2AA,TEMBA,TEMAB,V1,V2,
      4 TEM3BA,TEMBB,TEM2BB,TEM2AB,F,TEM2BA,TEM4BA,DNOM)
       IMPLICIT REAL (K,L,M)
       REAL*8 F,ICNT,INT,GN,D9,ACL
       REAL*8 SRE,SIM,CWI,CWR
       REAL*8 DLOG,DSORT,DATAN
       COMMON/T/TSAMP,CPOLES,CZEROS
       DIMENSION ICNT(NSTOT2),INT(NSTOT2),GN(NSTOT,NSTOT),D9(NSTOT2),
      1 CWR(NSTOT),CWI(NSTOT),TINV(NDIG,NDIG),ACL(NSTOT,NSTOT),
      2 RVEC(NSTOT,NSTOT),VECRN(NSTOT,NSTOT),VECIN(NSTOT,NSTOT),
      3 VECR(NSTOT,NSTOT),VECI(NSTOT,NSTOT),VRV(NSTOT),VIV(NSTOT),
      4 VPRV(NSTOT),VPIV(NSTOT),APRIME(NS,NS),BPRIME(NS,NC),
      5 P(NS,NS),Q(NS,NC),C1(NC,NS),C2(NC,NDIG),C3(NC,NS)
       DIMENSION M1(NDIG,NDIG),M2(NDIG,NDIG),M3(NDIG,NS),M4(NDIG,NS),
      1 M5(NDIG,NS),M6(NDIG,NS),A(NPLANT,NPLANT),B(NPLANT,NC),
      2 C(NACT,NACT),D(NACT,NC),TEM5BA(NDIG,NS),TEMAA(NS,NS),
      3 TEM2AA(NS,NS),TEMBA(NDIG,NS),TEMAB(NS,NDIG),V1(NSTOT2),
      4 V2(NSTOT2),TEM3BA(NDIG,NS),TEMBB(NDIG,NDIG),TEM2BB(NDIG,NDIG),
      5 TEM2AB(NS,NDIG),F(NSTOT,NSTOT),TEM2BA(NDIG,NS),TEM4BA(NDIG,NS)
      6 ,DNOM(NACT,NC)
CCCCC
CCCCC DIFFEQ IS A USER-WRITTEN PROGRAM THAT DETERMINES THE DIFFERENCE
CCCCC EQUATIONS USED IN THE DIGITAL CONTROL. MORE SPECIFICIALLY
CCCCC IT DEFINES THE MATRICES: M1,M2,M3,M4,M5,M6, AND C1,C2,C3
CCCCC IN TERMS OF TSAMP AND ANY CONTROL CONSTANTS. IT IS CALLED
CCCCC SEVERAL TIMES IN GETTING THE COMPENSATION (IMS=2) SO CONTROL
CCCCC PARAMETERS SHOULD NOT BE READ IN THE SUBROUTINE, BUT SHOULD
CCCCC INSTEAD BE READ AT THE BEGINNING OF THE PROGRAM AND PASSED
CCCCC TO DIFFEQ IN A LABELED COMMON. THE EQUATION OF THE
CCCCC COMPENSATION MUST BE PROGRAMMED HERE, AND THUS, NDIG, THE
CCCCC NUMBER OF DIFFERENCE EQUATIONS MUST INCLUDE THE COMPENSATION
CCCCC EQUATION.
CCCCC THE PROGRAM SHOWN HERE IS FOR THE LONGITUDINAL ATTITUDE
```

```
CCCCC CONTROL-WHELL STEERING PROBLEM DISCUSSED IN THE BODY OF THE
CCCCC REPORT
CCCCC
      EO16=EXP(-TSAMP/16.)
      EO16F3=57.29577951*(1.+FO16)/2.
      C2(1,3)=1.
C WASHOUT
      M1(1,1)=EO16
      M3(1,2)=-EO16F3*2.16
      M4(1,2)=EO16F3*2.16
C COMPENSATION
      TT2=EXP(-TSAMP*CPOLES)
      TT1=EXP(-TSAMP*CZEROS)
      M1(2,2)=TT2
      GLL=(1.-TT2)/(1.-TT1)
      M1(2,1)=-GLL*TT1
      M2(2,1)=GLL
      M3(2,3)=-GLL*TT1*247.53
      M4(2,3)=GLL*247.53
C DELAY
      M1(3,2)=1.
      RETURN
      END
```

The utility routines are:

MMULT	matrix multiplication
MADD	matrix addition
MATIN	matrix initialization (0 or I)
MATEQ	equate two matrices
SCAMAT	matrix-scaler multiplication
FGPQ	calculates φ given F
MINV	matrix inverse
CDIV	complex number division
HQR2	eigenvalue solver (QR algorithm)
BALANC	preprocesses matrix for HQR2
ELMHES	postprocesses matrix from HQR2

References

1. Deets, D. A., and Szalai, K. J., "Design and Flight Experience with a Digital Fly-by-Wire Control System Using Apollo Guidance System Hardware on an F-8 Aircraft," AIAA Paper No. 72-881, Aug. '72.

2. Mathews, Mark A., "SAAB Digital Flight Control," AIAA Paper No. 74-26, Feb. '74.

3. Edwards, J. W., " A Comparison of Digital Design Techniques for Digital Flight Control Synthesis," JACC June '73.

4. Lee, J. F. L., "A Digital Flight Control System Design Approach for a Space Shuttle Booster Type Vehicle," AIAA Paper No. 74-20, Aerospace Sciences Meeting, Feb. 1974.

5. Stubbs, G. S., Penchuk, A., Schlundt, R. W., "Digital Autopilots for Thrust Vector Control of the Apollo CSM/LM Vehicles," AIAA Paper No. 64-847, Aug. 1969.

6. Simmons, J. C. and Hall, B. M., "Digital Control System Development for the Delta Launch Vehicle," AIAA Paper No. 73-847, Aug. 1973.

7. Berman, H. and Gran, R., "An Organized Approach to the Digital Autopilot Design Problem," AIAA Paper No. 73-848, Aug. 1973.

8. Johnson, J. M., "The Application of Digital Filters Using Observers to the Design of an ICBM Flight Control System," AIAA Paper No. 73-845, Aug. 1973.

9. Powell, J. D., and Katz, P., "Sample Rate Selection for Aircraft Digital Control," AIAA J, August 1975.

10. Borow, M. S., et al., "Navy Digital Flight Control System Development," Honeywell Document No. 21857-FR, Honeywell, Inc., Minneapolis, Minn., Dec. 1972.

11. Sutton, M. L., "Feasibility Study for an Advanced Digital Flight Control System," LSI Tech. Report No. ADR-773, Lear-Siegler, Inc., Santa Monica, CA., Oct. 1972.

12. Konar, A. F., et al., "Digital Flight Control Systems for Tactical Fighters," Report No. AFFDL-TR-73-119, by Honeywell, Inc. for the A.F. Flight Dynamics Laboratory, Dec. '73.

13. Rader, C.M., Rabiner, L. R., Digital Signal Processing IEEE Press, 1972.

14. Huelsman, L. P., Active Filters, McGraw-Hill, 1970.

15. Edwards, J. W., "A Comparison of Digital Design Techniques for Digital Flight Control Synthesis", tutorial, NASA Flight Research Center, Memorandum.

16. Slater, G. L., "A Unified Approach to Digital Flight Control Algorithms", AIAA Paper No. 74-884, August 1974.

17. Tuttle Jr., David F., Network Synthesis, Vol. 1 John Wiley & Sons, 1958.

18. Bryson, Jr., A.E.,"Control Theory for Random Systems" SUDAAR No. 447, September 1972.

19. Bryson, Jr., A. E., Hall, W. E.,"Optimal Control and Filter Synthesis by Eigenvector Decomposition" SUDAAR No. 436, November 1971.

20. Katz, Paul and Powell, J. D., "Selection of Sampling Rate for Digital Control of Aircraft". SUDAAR No. 486, September 1974. Stanford University, Aero/Astro Dept.,